Theory of excitation-contraction coupling in cardiac muscle

Michael D. Stern
Division of Cardiology, 592 Carnegie Building, The Johns Hopkins Medical Institutions, Baltimore, Maryland 21205; and
Gerontology Research Center, National Institute on Aging, National Institutes of Health, Baltimore, Maryland 21224 USA

ABSTRACT The consequences of cardiac excitation-contraction coupling by calcium-induced calcium release were studied theoretically, using a series of idealized models solved by analytic and numerical methods. "Common-pool" models, those in which the trigger calcium and released calcium pass through a common cytosolic pool, gave nearly all-or-none regenerative calcium releases (in disagreement with experiment), unless their loop gain was made sufficiently low that it provided little amplification of the calcium entering through the sarcolemma. In the linear (small trigger) limit, it was proven rigorously that no common-pool model can give graded high amplification unless it is operated on the verge of spontaneous oscillation. To circumvent this problem, we considered two types of "local-control" models. In the first type, the local calcium from a sarcolemmal L-type calcium channel directly stimulates a single, immediately opposed SR calcium release channel. This permits high amplification without regeneration, but requires high conductance of the SR channel. This problem is avoided in the second type of local control model, in which one L-type channel triggers a regenerative cluster of several SR channels. Statistical recruitment of clusters results in graded response with high amplification. In either type of local-control model, the voltage dependence of SR calcium release is not exactly the same as that of the macroscopic sarcolemmal calcium current, even though calcium is the only trigger for SR release. This results from the existence of correlations between the stochastic openings of individual sarcolemmal and SR channels. Propagation of regenerative calcium-release waves (under conditions of calcium overload) was analyzed using analytically soluble models in which SR calcium release was treated phenomenalogically. The range of wave velocities observed experimentally is easily explained; however, the observed degree of refractoriness to wave propagation requires either a strong dependence of SR calcium release on the rate of rise of cytosolic calcium or localization of SR release sites to one point in the sarcomere. We conclude that the macroscopic behavior of calcium-induced calcium release depends critically on the spatial relationships among sarcolemmal and SR calcium channels, as well as on their kinetics.

INTRODUCTION

The cardiac contraction is coordinated by an electrical action potential propagated throughout the cardiac syncytium. Despite many years of research, the exact mechanism by which this electrical signal is transduced into contraction of the myofilaments is not understood. The broad outlines of the process are known: depolarization of the sarcolemma causes influx of calcium through voltage-dependent channels; a larger amount of stored calcium is then released from the sarcoplasmic reticulum (SR). The released calcium, together with the calcium entering through the sarcolemma, binds to troponin-C and activates the myofilaments. In the past few years, calcium channels, which are believed to mediate calcium release from the SR, have been isolated from the sarcoplasmic reticulum.

The exact nature of the trigger signal which activates these SR calcium channels is not known. In skeletal muscle, a large body of evidence indicates that charge movements induced by depolarization of the sarcolemma are communicated directly to the SR channel. In cardiac muscle, on the other hand, the preponderance of the evidence indicates that the depolarization of the sarcolemma plays no direct role in the control of SR calcium release; release of SR calcium is triggered by the calcium that enters the cell via the voltage-controlled calcium channels in the sarcolemma. This hypothesis, known as "calcium-induced calcium release", is the basis of the theoretical analysis presented here.

The experimental evidence in favor of calcium-induced calcium release will be reviewed only briefly here; a more detailed review has been given by Fabiato (1989). In intact cardiac myocytes, the cardiac calcium transient is abolished if extracellular calcium is removed, even during a single beat (Nabauer et al., 1989). A similar suppression of calcium release is found if the inward calcium current is blocked by dihydropyridines (Wier and Yue, 1985) or by depolarizing the voltage-clamped sarcolemma to the calcium reversal potential (Cannell et al., 1987; Barcenas-Ruiz and Wier, 1987). Intracellular liberation of free calcium by photolysis of caged calcium triggers release of SR calcium in a manner independent of membrane potential (Niggli and Lederer, 1990). Calcium entering through sarcolemmal calcium channel tail currents can trigger release of calcium after the cell has been repolarized to the resting potential. All these facts imply that it is the trans-sarcolemmal calcium flux, rather than the depolarization of the sarcolemma, per se, that triggers SR calcium release.

In order to study the details of CICR, Fabiato (1983, 1985*a, b, c*) carried out an ingenious series of experiments in which mechanically skinned cardiac myocytes were superfused with solutions containing various concentrations of free calcium, in a system permitting solu-

Address correspondence to Michael Stern at The Johns Hopkins Medical Institutions.

tion change within 1 ms; released calcium was measured either with aequorin bound to the myofilaments, or by calibration of myofilament tension. Rapid increase of bathing $[Ca^{2+}]$ to levels above 100–150 nM (depending on species) provoked release of SR calcium. The amount of calcium released increased with trigger $[Ca^{2+}]$ in a smoothly graded manner up to an optimum trigger level (560 nM in the rat myocyte, 3 μM in the dog Purkinje cell). Higher triggers produced less release; above a trigger $[Ca^{2+}]$ of 10 μM release was almost completely prevented, so that the peak $[Ca^{2+}]$ produced at the myofilaments was much less than that of the trigger solution itself. The magnitude of triggered release was very sensitive to the rate of rise of trigger $[Ca^{2+}]$; a rapid rise caused release, whereas a slow rise caused uptake into the SR. Application of high $[Ca^{2+}]$ could partially inhibit a release which was already in progress, if it was applied early enough, but sustained application of an inhibiting $[Ca^{2+}]$ resulted, after a delay, in the appearance of repetitive "spontaneous" calcium releases.

These results make it clear that there is a sensitive calcium-induced calcium release process, as well as some kind of calcium-dependent inactivation of release. A quantitative, mechanistic interpretation of these experiments is not simple, because calcium in the myofilament space is not clamped (else it would not be possible to observe the release), and, even at the outer face of the SR, the surrounding solution provides sufficient diffusion resistance to permit the development of calcium gradients during the period when the injected droplet remains unstirred. Efforts to make these observations the basis of a quantitative theory of calcium release in the intact cell have so far been unsatisfactory, as described below.

There have been a number of published efforts to model cardiac calcium-induced calcium release over the past several years (Hilgemann and Noble, 1987; Wong et al., 1987; Wong, 1981; Adler, et al., 1985; Kauffmann et al., 1974) and other extensive efforts that have not been published in full (Stern et al., 1984; Schouten et al., 1988; M. Cannell, personal communication). This work has aimed at quantitative simulation of the detailed behavior of skinned or intact cells under particular sets of experimental conditions. These models have required departures from pure calcium-induced calcium release, or other ad-hoc features in order to fit details of particular experiments, and have generally required major revision to cope with new experimental findings. The two most highly developed modeling efforts are those of Hilgemann and Noble (1987), and of Wong et al. (1987).

The Hilgemann model is an extension of the action-potential model of DiFrancesco and Noble (1985), incorporating more detailed modeling of intracellular calcium handling. In this model, calcium release is controlled by a nonlinear function of a state variable which is in turn controlled by a system of three differential equations, with activation and inactivation by calcium, as well as direct activation by an exponential function of sarcolemmal membrane potential. This complicated scheme was arrived at after extensive trials of 20 different calcium-induced calcium release mechanisms. It was found to be impossible to simulate the experimental results of Fabiato by any of these schemes, and the inclusion of direct voltage-dependent activation (which is increasingly in conflict with the experimental evidence) was needed in order to reproduce the presence of smoothly graded SR calcium release over a wide range of sarcolemmal calcium current. It should be noted that the models considered in this search were all of the class which we refer to as "common-pool" models (see below), meaning that the trigger calcium reaches the SR via the same cytosolic calcium pool into which SR calcium is released.

The Wong model was designed expressly for the purpose of reproducing the results of Fabiato's experiments. In this model, an "appositional space" is assumed to communicate freely with the outer surface of the SR (and with the bathing medium, in the case of a skinned cell). The myofilaments, in contrast, are in a "sarcoplasmic space" that receives calcium only from the "release terminal", a compartment that receives calcium either by active (pump) reuptake from the sarcoplasmic space, via the longitudinal SR, or from the body of the SR by passive diffusion. The most notable feature of this model is that release from the release terminal is controlled by a product of activation and inactivation factors which are functions of both appositional and sarcoplasmic calcium. Because of the control of release by trigger calcium in a compartment different from that into which release occurs, the model is not a common-pool model, in the sense used in this article. The physical mechanism for this "action at a distance," by means of which the release channel is controlled by calcium in a different compartment, is not specified; presumably a second messenger within the SR would be required. In view of the difficulty that many investigators have experienced in finding simple or physically plausible mechanisms that could reproduce the experimental data, we believe that the construction of a global model capable of simulating a cell in quantitative detail is premature. We have taken a different philosophical approach in this work, studying a number of partial models designed to show, in a qualitative but mathematically well defined way, how the microscopic properties of calcium-induced calcium release translate into macroscopic physiologic phenomena, which is often not intuitively obvious. Modeling is therefore used as an aid to understanding of alternative hypotheses, rather than an attempt to simulate the behavior of the cell in full detail.

COMMON-POOL MODELS

In modeling calcium-induced calcium release, it has usually been assumed that there is one cytosolic pool of

calcium, whose concentration controls the release of calcium from the SR, and into which the calcium from both the SR and the sarcolemmal calcium current enter (Fig. 1; note that there could be other calcium pools not shown, so long as the release of calcium from the SR is controlled by $[Ca^{2+}]$ in the cytosolic pool into which SR calcium is released). Such an arrangement has obvious positive feedback, suggesting that it might produce an "all-or-none" response; SR calcium release, once triggered by calcium crossing the sarcolemma, would escape from sarcolemmal control and evolve autonomously.

It has been known for many years (New and Trautwein, 1972) that contraction amplitude is a smoothly graded function of membrane potential during voltage clamp depolarizations. The development of calcium sensitive intracellular fluorescent probes has made it possible to map the relationship between membrane potential and cytosolic calcium in detail. There is now abundant evidence (Cleemann and Morad, 1991; Talo, 1990; Beucklemann and Wier, 1988; Cannell et al., 1987) that normal SR calcium release is smoothly graded as a function of the calcium trigger provided by the slow inward current. If the magnitude of the calcium transient is plotted as a function of membrane potential during a step depolarization of constant duration, a bell-shaped curve is obtained which resembles the curve of peak or integrated sarcolemmal calcium current measured from the same cell. On the other hand, if the inward calcium current is terminated early, either by repolarizing the cell to the holding potential, or by depolarizing further to the calcium reversal potential, calcium release from the SR is also terminated. There is therefore no experimental evidence that SR calcium release becomes autonomous under these conditions.

On the other hand, when cells are "calcium loaded" they produce spontaneous calcium oscillations due to release of calcium from the SR, and these "spontaneous" calcium releases can propagate throughout the cell as a wave of calcium release. These are phenomena that might be expected from a regenerative calcium-induced calcium release mechanism, and, indeed, they are suppressed by ryanodine, which blocks the SR calcium release channel in a partially open state and depletes the SR of calcium (Rousseau et al., 1987). Fabiato (1985*d*) has argued that spontaneous calcium release is not the same phenomenon as calcium-induced calcium release. In particular, in a "normally" calcium loaded skinned myocyte, calcium-induced calcium release requires a rapid rise of applied $[Ca^{2+}]$; a gradual rise will cause loading of the SR rather than release. Rapid application of high concentrations of calcium will suppress a calcium release that is in progress, whereas sustained application of high calcium results in spontaneous release, after a delay to permit loading of the SR. Further, spontaneous releases appears to originate at the nadir of cytosolic calcium concentration. However, both processes appear to involve the same SR calcium pool and release channel, as judged by the response to caffeine, ryanodine and ruthenium red, and spontaneous release, once initiated at one point in the cell, propagates as a wave, indicating that some aspect of the "spontaneous" release process is capable of triggering release from adjacent SR. All published models of calcium-induced release (as well as unpublished ones that are known to the author) display spontaneous oscillation under conditions of high calcium loading. We will therefore assume in this study that calcium oscillations and propagated waves of calcium release are manifestations of regeneration of a calcium-induced calcium release mechanism, although, in the present state of the evidence, this is a somewhat arbitrary choice.

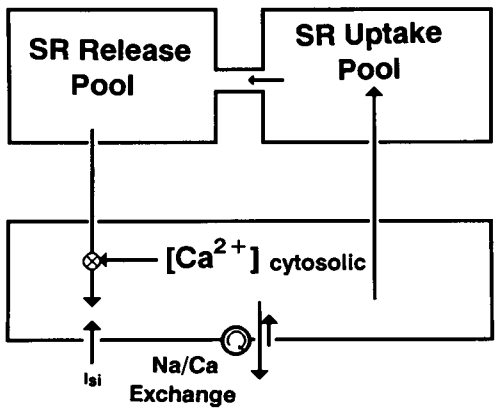

FIGURE 1 Schematic of common-pool calcium models. All calcium entering or leaving the cell or organelles passes through a common cytosolic free-calcium pool. The concentration of free calcium in this pool controls the release of calcium from the SR calcium-induced calcium release channels.

To date, no common-pool model capable of reproducing the graded calcium release (in response to depolarization) observed experimentally has been put forward. Extensive efforts to accomplish this were unavailing (Hilgemann and Noble, 1987; D. Hilgemann, personal communication). The author's experience over ten years of modeling has been similar. While space does not permit the explicit display of numerous common pool models that do not work, the experience with such models can be qualitatively summarized. Models with a high "loop gain", i.e., a calcium release mechanism highly sensitive to cytosolic calcium, produce all-or-none calcium transients that evolve autonomously once cytosolic calcium has been raised above a threshold by a calcium trigger. Models with low loop gain produce only modest augmentation and prolongation of the calcium transient over that which would be produced by the trigger calcium alone. If the loop gain is adjusted critically, it is possible to get significant graded amplification of the transient, but such gradation is generally quite nonlinear, and is associated with prolongation and shape change of the transient as the trigger size is varied. Com-

mon pool models tend to "latch-up" in a state where SR release is continuous, unless a mechanism is provided to interrupt release. Either calcium- and time-dependent inactivation of the release channel, or depletion of a slowly replenished release store can prevent this problem. In order to simulate the observed stable resting state, combined with the possibility of triggering a large increase in cytosolic calcium by means of a small trigger (i.e., one which would not, by itself, raise cytosolic calcium by an amount large compared to resting calcium), it is necessary to use a release mechanism that has a nonlinearity of at least second degree; this is also necessary to produce a system that displays spontaneous oscillations when resting calcium is raised. The present, limited data on control of the SR calcium release channel indicate that the steady-state open probability has a linear or sublinear dependence on cytosolic calcium (Meissner and Henderson, 1987; Rousseau and Meissner, 1989; Ashley and Williams, 1990).

It is not possible to prove that no common-pool model can fit the observations, because there is an unlimited variety of possible common-pool models that could be devised. However, the experimental evidence suggests that SR calcium release is a smoothly graded function of the trigger amplitude down to arbitrarily small triggers. If this is so, SR calcium release can be studied in the linear regime in which the trigger is made sufficiently small that the cell remains near its equilibrium point and behaves in a linear manner. Because all linear systems can be classified systematically, it is possible to make rigorous statements relating the magnitude of amplification by SR calcium release to the stability of the cell against spontaneous oscillations. The power of this analysis is that it applies to any common-pool model whatever; no specification of the details of release or uptake mechanisms are required.

Linear stability theory of common-pool models

Assume that the cell rests in a stable equilibrium configuration with a cytosolic calcium $[Ca^{2+}]_{equ}$, and that it is perturbed within a range over which its behavior is linear (if the equilibrium is stable, this should be possible). The departure of cytosolic calcium from equilibrium will be described by the variable $X \equiv [Ca^{2+}]_{cyto} - [Ca^{2+}]_{equ}$. In the most general possible common-pool model, there are three contributions to the rate of change of X: entry of trigger calcium at a rate $I(t)$, release of calcium into the cytosol at a rate $R\{x(t)\}$, and uptake of calcium from the cytosol at a rate $U\{x(t)\}$. The release and uptake functionals $R\{\ \}$ and $U\{\ \}$ are "black boxes" that determine the release and uptake calcium fluxes as a function of the past history of the cytosolic calcium $x(t)$. All that will be assumed about these black boxes is that they are stable and physically realizable, and that they are time-stationary, i.e., they have no external clock or permanent memory.

It is well known from linear systems theory that the most general (linear) time-stationary response functional (i.e., "black box" response) is obtained by convoluting the input with a kernel function that describes the weighting of the contributions of past values of the input to the output. This follows from linearity because the output can be obtained by adding up the "impulse responses" of the system to all past inputs; because of time stationarity, the impulse response is the same regardless of the time of the input. Therefore, the linearized evolution of (the departure from equilibrium of) cytosolic calcium in the most general possible common-pool model can be described by the following equation:

$$V\frac{dX}{dt} = -\int_0^t U(t-t')X(t')\,dt' + \int_0^t R(t-t')X(t')\,dt' + I(t), \quad (1)$$

where V is the effective volume of the cytosolic pool, and $R(t)$ and $U(t)$ are the kernels (impulse response functions) of the release and uptake "black boxes".

The strategy of the analysis will now be as follows. Imagine a thought experiment in which a cell is triggered to produce a cytosolic calcium transient, giving curve A in Fig. 2. The experiment is then repeated with the release machinery "turned off" (for example by use of ryanodine) giving the much smaller transient in curve B. Qualitatively, curve A represents the total cytosolic calcium obtained when the release machinery sees curve A as the net trigger, while curve B represents the contribu-

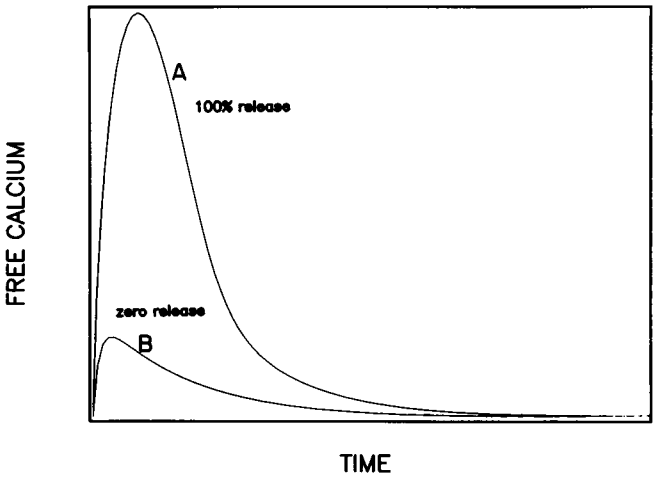

FIGURE 2 Hypothetical results of a thought-experiment in which a calcium transient is measured under normal conditions (A) and after turning off SR calcium release (B), with the same trigger calcium. Under linear conditions, a common-pool model can only give such a result (showing a dominant contribution of SR calcium release) if the cell is on the verge of spontaneous oscillation (see text). Horizontal axis is time, vertical axis is $[Ca^{2+}]$, units arbitrary.

tion of the inward current to this total. The difference $A - B$ is the contribution of SR calcium to the total, self-consistent trigger. If A is much larger than B (i.e., if a large amplification is obtained from SR release), then $A - B$ will be almost as large as A, i.e., the release is almost large enough to serve as its own trigger, which would permit it to be self-sustaining. Then, a slight increase in the gain of the release process would make it self-sustaining, i.e., the cell must be on the verge of spontaneous oscillation. This argument is made mathematically rigorous by solving Eq. 1 formally by Laplace transform methods to calculate the largest factor by which the gain of the release process could be increased before instability would set in (safety margin for stability).

Recall the definition of the Laplace transform of a function of time:

$$x(s) = \int_0^\infty X(t)e^{-st}\,dt, \tag{2}$$

which expresses the function in the "frequency domain" as a function of the complex frequency variable s. Taking the Laplace transform of Eq. 1, we obtain:

$$sx(s) = -\frac{u(s)x(s)}{V} + \frac{R(s)x(s)}{V} + \frac{i(s)}{V}, \tag{3}$$

which is a purely algebraic equation. This may be solved for the Laplace transform of the cytosolic calcium transient:

$$x(s) = \frac{i(s)}{sV + u(s) - R(s)}. \tag{4}$$

Alternatively, we may assume that $x(t)$ is known from experiment (curve A in Fig. 2), and solve Eq. 3 for $R(s)$, the Laplace transform of the release functional:

$$R(s) = \frac{sx(s)V + u(s)x(s) - i(s)}{x(s)}. \tag{5}$$

Next, we determine what new calcium transient x_N would result if the release process were modulated by multiplying it by the constant r. This is obtained by multiplying Eq. 5 by r, and inserting the result into Eq. 4 in place of R:

$$x_N(s) = \frac{i(s)}{-r(x(s)(sV + u(s)) - i(s))/x(s) + sV + u(s)}. \tag{6}$$

One particular case of "modulation" would be to turn release off entirely, by setting $r = 0$, giving the Laplace transform x_0 of curve B in Fig. 2:

$$x_0(s) = \frac{i(s)}{sV + u(s)}. \tag{7}$$

Since curve B is known from "experiment", we can solve this equation to find the unknown trigger $i(s)$:

$$i(s) = x_0(s)(sV + u(s)). \tag{8}$$

Now suppose, instead, that the "modulation" consists of increasing the gain of the release process above normal by using $r > 1$. Eventually this will lead to spontaneous instability due to regeneration. The general criterion for stability of a system in the complex frequency domain is that its response should have no poles with positive real parts (which correspond to modes which increase exponentially with time). The poles of the right hand side of Eq. 6 are simply the values of s at which its denominator is zero, which (substituting from Eq. 8 for $i(s)$) are determined by:

$$x(s)(1 - r) + rx_0(s) = 0. \tag{9}$$

Under normal conditions ($r = 1$) these poles all have negative real parts, because the cell is postulated to be stable at rest. These poles may be pictured as points in the left half of the complex plane. As r is increased above 1, the poles will move rightward. When one of them crosses the imaginary axis into the right half-plane, then instability sets in. In particular, if a pole on the real axis crosses into the right half-plane, it will pass through the point $s = 0$. Therefore, if r is increased until $s = 0$ becomes a solution of Eq. 9, the cell will certainly have become unstable; in fact, in the presence of a pole at $s = 0$, it will be statically unstable, able to self-sustain an arbitrary constant displacement of cytosolic calcium from equilibrium. By inserting $s = 0$ into Eq. 9 and solving for r, we find the maximum factor by which release could be increased before (static) instability must result (instability due to some other pole could occur at even smaller values of r):

$$r_{crit} = \frac{1}{1 - \frac{x_0(0)}{x(0)}}. \tag{10}$$

By the definition of the Laplace transform, Eq. 2, $x(0)$ and $x_0(0)$ are simply the areas under curves A and B in Fig. 2. Eq. 10 gives the maximum "safety factor" by which we might be able to increase the gain of release before incurring instability, as a function of the ratio of these two areas. A numerical example illustrates the point. If curve A has 10 times the area of curve B, then $r_{crit} = 1.11$. If the gain of release were increased by only 11% (e.g., by increasing SR calcium loading), then the cell would oscillate.

While it is conceivable that cells somehow self-regulate their release gain in order to remain on the border of instability, this is not a robust mechanism, because small variations of parameters will easily lead to instability. It would be surprising if nature required the fine tuning of a barely stable positive feedback loop in order to control

SR calcium release in a graded manner. It seems more likely that common-pool models of calcium-induced calcium release cannot explain cardiac excitation-contraction coupling. In order to rule out all common-pool models experimentally, it would be necessary to study cells in a clearly linear regime (e.g., where the magnitude of the calcium transient is small compared with resting calcium), and to show that high amplification was present over a wide range of release gain (e.g., wide variation of SR loading).

LOCAL CONTROL MODELS

In order to resolve the paradox of graded calcium-induced calcium release, what is needed is a mechanism which will break the positive feedback loop by separating the calcium released by the SR from the calcium that acts as the trigger controlling the SR release channel. One way of doing this is suggested by the ultrastructural architecture of the SR calcium release terminals. In skeletal muscle, it is well established that the SR release channels are in direct apposition to dihydropyridine (DHP) receptors in the sarcolemma of the t-tubule, which act as voltage sensors and at least some of which are functioning L-type calcium channels (Block et al., 1988). Whereas the exact ultrastructural relation between the sarcolemmal and SR calcium channels in cardiac muscle has not been demonstrated, it is known that the DHP and ryanodine receptors co-purify in a junctional membrane fraction (Wibo, 1991), and it is generally believed that there is a close relationship. This would give the calcium passing through the L-type calcium channel a privileged access to the calcium-sensing site on the SR channel. The calcium sensitivity of this site could then be much less than the ambient cytosolic calcium level, preventing regenerative calcium release. A simple model embodying these ideas is the "calcium-synapse" model shown schematically in Fig. 3.

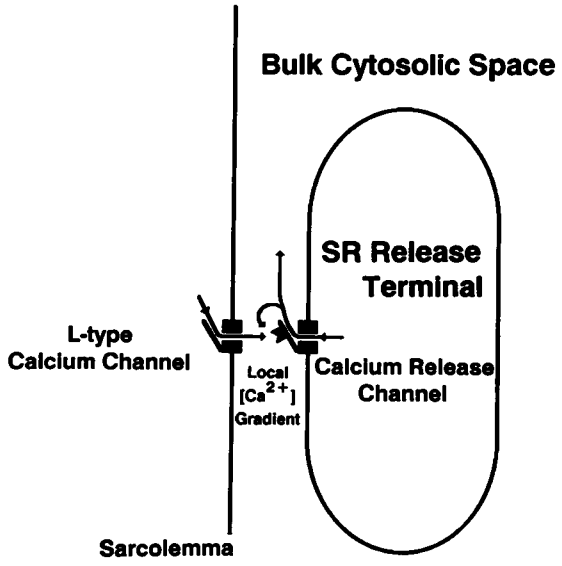

FIGURE 3 Schematic of the "calcium-synapse" model, in which each SR release channel is immediately opposite a sarcolemmal L-type calcium channel, and is directly controlled by the local calcium released from that channel.

It might appear that this model would only transfer the regeneration problem to a smaller space. Since the SR channel would have low calcium sensitivity, bulk regeneration of cytosolic calcium would not occur, but each SR channel could still sense the calcium which it, itself, released. Since the SR release channel is only 34 nm in diameter (Lai et al., 1988), the calcium feedback would again be as large or larger than the local trigger from the sarcolemmal channel. The SR channel, once open, would "latch up" in response to its own calcium release and remain open, independent of further control by the sarcolemma. This does not occur because the all-or-none nature of single channel openings, combined with the short diffusion times in the small space around the channels, prevents regeneration, as explained below.

Calcium gradients in the neighborhood of a channel

We first calculate the calcium concentration in the neighborhood of a single calcium channel (either sarcolemmal or SR) lying in a (locally) planar lipid membrane. We will initially ignore calcium buffering, because most of the cytosolic buffer sites are fixed on myofilaments or other membranes or organelles that will probably not be present in the small region around the sarcolemmal and SR channel molecules. We treat the channel pore as a point source from which calcium issues at a flux rate s (mol/s). The calcium concentration C in the region around the channel is governed by the diffusion equation:

$$\frac{\partial C}{\partial t} = D\left(\frac{\partial^2 C}{\partial z^2} + \frac{\partial^2 C}{\partial y^2} + \frac{\partial^2 C}{\partial x^2}\right). \tag{11}$$

When the channel has been open for some time, the free calcium distribution in the neighborhood of the channel will be given by the steady-state solution of Eq. 11 for a point source, which is well known to be:

$$C_0 = \frac{s}{2\pi Dr} = \frac{s}{2\pi D(z^2 + y^2 + x^2)^{1/2}}. \tag{12}$$

The factor 2 (rather than 4) in the denominator accounts for the fact that all the calcium issuing from the pore goes to the cytosolic side of the membrane, unlike a true isotropic point source. Supposing that the channel closes at time $t = 0$, the calcium distribution around the channel will be the solution of the source-free diffusion Eq. 11, with Eq. 12 as an initial condition. This solution is found by spatially convoluting the initial concentration (of Eq. 12) with the Green's function for Eq. 11,

which is the Gaussian solution of Eq. 11 describing the diffusion of calcium initially localized at a point. The result is:

$$C = \frac{S\,\mathrm{erf}\left\{\frac{r}{2(Dt)^{1/2}}\right\}}{2\pi Dr}, \qquad (13)$$

for the concentration of free calcium at a distance r from the channel pore, at time t after the channel closure.

Eq. 15 is plotted in Fig. 4. Panel B shows $[Ca^{2+}]$ as a function of distance from a channel passing 2 picoamperes of calcium current at times of 0.01, 0.1, 1, 10, and 100 μs after the channel closes. Panel A shows the same data as a function of time at distances of 10, 30, and 100 nm from the pore. The significant point is that there is a large local excess concentration of calcium above ambient cytosolic levels when the channel is open, and this excess dissipates within a fraction of a millisecond after the channel closes.

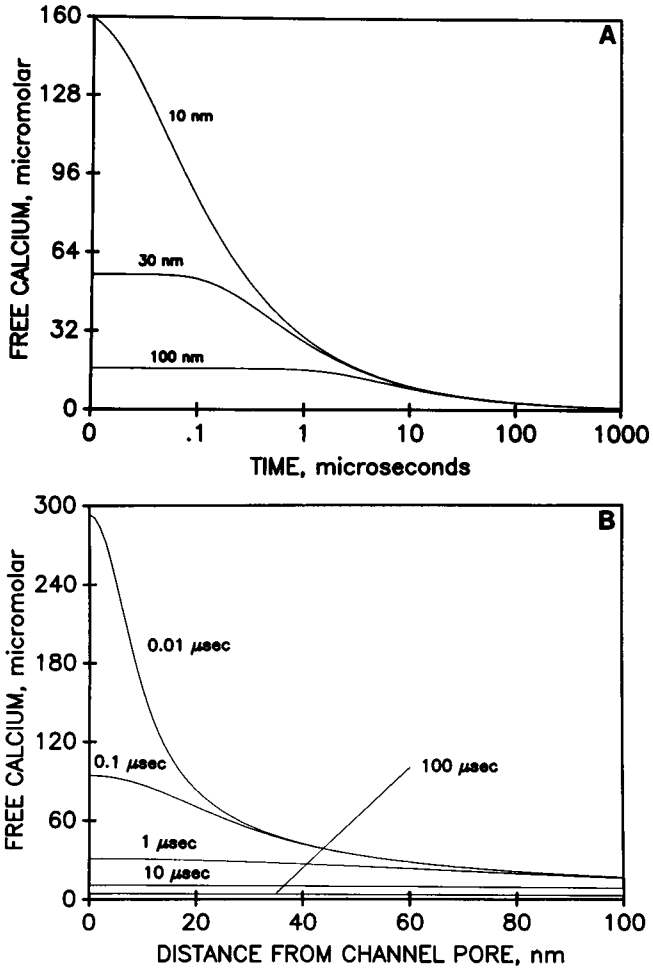

FIGURE 4 Free calcium concentration in the neighborhood of a channel pore immediately after the channel closes. The channel was conducting a calcium current of 2 picoamperes until time $t = 0$, at which time it closed, leaving the local calcium gradient to decay by diffusion. (A) $[Ca^{2+}]$ as a function of time at distances of 10, 30, and 100 nm from the channel pore. (B) $[Ca^{2+}]$ as a function of distance from the channel pore at 0.01, 0.1, 1, 10, and 100 μs after channel closure.

Analysis of the "calcium-synapse" model

Consider, now, the model in Fig. 3. Depolarization of the sarcolemma will cause the L-type channel to open, resulting, within microseconds, in a steady high concentration of calcium at the calcium sensing site of the SR channel, which is presumed to be closed. This will cause the SR channel to open, resulting in an even higher local concentration of calcium. There are now two possibilities. If the open state of the channel is calcium insensitive (as suggested by the data of Ashley and Williams [1990] from single SR sheep purkinje SR channels in lipid bilayers), then the SR channel will close at random. Provided this closure lasts longer than a fraction of a millisecond, the local calcium gradient will dissipate, and the SR channel will remain closed for a prolonged period unless the L-type channel is still delivering trigger calcium. If, on the other hand, the open state lifetime of the SR channel is calcium dependent (as indicated by the data of Rousseau and Meissner [1989] from dog ventricular channels), the open channel, which sees a very high calcium, will close at a slower, but still finite rate. Once it has closed, the self-calcium gradient will dissipate, and the channel will, again, remain closed unless stimulated by calcium from the L-type channel. In either case, the stochastic closings of the single channel will interrupt the positive feedback loop, so that the probability of the SR channel being open will be closely coupled to the open probability of the sarcolemmal L-type channel, giving graded calcium release from the SR. The only difference between the two cases is that, in the case of the calcium-sensitive open state, the open lifetime will depend on $[Ca^{2+}]$ at the SR channel. Since the major contribution to local $[Ca^{2+}]$ is the calcium issuing from the open SR channel itself, the variation of the open lifetime due to the calcium from the sarcolemmal channel (let alone the ambient cytosolic calcium) will be a secondary effect. For purposes of qualitative modeling, then, we may assume that the open state is calcium insensitive. An additional detail is the possibility that, even if the open state of the SR channel is calcium insensitive, the calcium binding site may be available for occupancy. In that case, the rate limiting step in breaking the positive feedback loop may be the time required for calcium to dissociate from this site, rather than the diffusion times shown in Fig. 4. If the calcium binding site has an on-rate that is diffusion limited, and an affinity that is comparable to the local concentration of calcium reached when the channels are open, then this dissociation time will be comparable to the diffusion times, and the argument remains essentially the same.

In order to analyze the "calcium-synapse" model quantitatively, it is necessary to take into account that

the openings of both the sarcolemmal and SR calcium channels are stochastic processes, which will be correlated because of their interaction. It is therefore necessary to analyze the model as though the pair of channels were a single channel, i.e., to consider all possible simultaneous states of the two channels, and the processes by which transitions may occur among them. The simplest possible calcium-synapse model is obtained by assuming that the SR channel has two states, open and closed, with the opening rate of the closed channel proportional to local $[Ca^{2+}]$ and the closing rate of the open channel independent of calcium. The sarcolemmal channel is assumed to have an activation gate and an inactivation gate, each obeying first order voltage-dependent kinetics (for computational purposes we assumed the model of DiFrancesco and Noble [1985] without the calcium-dependent inactivation). To make computation tractable, we assumed that the diffusional calcium changes (e.g., Fig. 4) are essentially instantaneous, so that the local excess $[Ca^{2+}]$ is determined by Eq. 12 when the channel(s) are open and zero otherwise. The unitary current of the SR channel was assumed to be a constant (i.e., effects of SR depletion, etc., were not included), whereas the unitary calcium current of the sarcolemmal channel had the usual voltage dependence, taken from the model of DiFrancesco and Noble. Uptake of calcium from the cytosol was modeled by a simple first order process.

Evaluation of the possible state-pair transitions leads to the following set of differential equations governing cytosolic calcium:

$$\frac{dF}{dt} = \alpha_F(1 - F) - \beta_F F$$

$$\frac{dD}{dt} = \alpha_D(1 - D) - \beta_D D \qquad (14a)$$

$$\frac{dI_r}{dt} = -I_r(r_c + CAk_0) - Ai_u i_{ur} k_o N P_{oo} + ADFi_u i_{ur} k_o N + CAi_{ur} k_o N$$

$$\frac{dP_{oo}}{dt} = -P_{oo}\left(r_c + Ai_u k_o + CAk_o + \frac{\beta_F DF + \beta_D DF}{DF} + \frac{\alpha_D(1 - D)F + \alpha_F D(1 - F)}{1 - DF}\right) + \frac{(\alpha_D(1 - D)F + \alpha_F D(1 - F))I_r}{(1 - DF)i_{ur}N} + DF(Ai_u + CA)k_o$$

$$\frac{dCA}{dt} = -\frac{(D_0F_0 - DF)i_u N - (CA_0 - CA)K + I_{r0} - I_r}{B},$$

where $D(t)$ and $F(t)$ are open probabilities of the activation and inactivation gates of the sarcolemmal channel, $CA(t)$ is (bulk) cytosolic $[Ca^{2+}]$, $I_r(t)$ is the (ensemble averaged) rate of calcium release from the SR and $P_{oo}(t)$ is the probability that both sarcolemmal and SR channels are simultaneously open (this variable carries the information about correlation between the openings of the two channels). In these equations, α_D, β_D, α_F, and β_F are the voltage dependent rate constants of the activation and inactivation gates of the sarcolemmal channel, and i_u is the unitary current of the sarcolemmal channel, given by (DiFrancesco and Noble, 1985):

$$i_u = \frac{(E - 50.0)(CAe^{100.0/E_0} - CA_o e^{-2.0(E-50.0)/E_0})P}{1 - e^{-2.0(E-50.0)/E_0}} \qquad (14b)$$

$$\alpha_D = \frac{30.0(E + 24.0)}{1.0 - e^{-0.25(E+24.0)}} \quad \beta_D = \frac{12.0(E + 24.0}{e^{0.1(E+24.0)} - 1.0}$$

$$\alpha_F = \frac{6.25(E + 34.0)}{e^{0.25(E+34.0)} - 1.0} \quad \beta_F = \frac{50.0}{e^{-0.25(E+34.0)} + 1.0}.$$

The constants i_{ur}, r_c, k_o, and N are the unitary current of the SR channel (note that, in this simple version of the model, the unitary current is a constant, i.e., we do not consider its possible variation with SR membrane potential or SR calcium concentration), the SR channel closure rate, the SR channel opening rate coefficient (i.e., k_o is multiplied by the local calcium concentration to obtain the opening rate), and the density of channel pairs, respectively. The constant A is the coefficient which converts unitary calcium currents to local calcium concentration at the sensing site of the SR channel. A is of the order of magnitude of $1/(2\pi D_{free} d)$ where D_{free} is the diffusion coefficient of free calcium and d is the distance between the sarcolemmal channel pore and the SR channel sensing site (see Eq. 12; the exact value of A depends on the geometry of the confined space between the channels). The constant K is a relaxation rate which represents the effect of SR and sarcolemmal pumps (and Na/Ca exchange), B is the relative effective volume of the cytosolic calcium space (i.e., it represents the effect of calcium buffering, considered as a fast, linear process), and CA_o and CA_0 are the extracellular and intracellular resting (at the holding potential) free calcium concentrations.

The differential equations (14a) are subject to the following equilibrium initial conditions evaluated at the holding potential:

$$I_{r0} = (((AD_0^2F_0^2 - AD_0F_0)i_u + CA_0D_0F_0 - CA_0)i_{ur}k_oNr_c + (((ACA_0D_0F_0 - ACA_0)i_u + CA_0^2D_0F_0 - CA_0^2)i_{ur}k_o + (((A(\beta_F + \beta_D + \alpha_F + \alpha_D)D_0^2 - A\alpha_D D_0)F_0 + (A(-\beta_F - \beta_D)D_0 - A\alpha_F D_0^2)F_0)i_u + ((\beta_F + \beta_D + \alpha_F + \alpha_D)CA_0D_0 - \alpha_D CA_0)F_0 - \alpha_F CA_0D_0 + (-\beta_F - \beta_D)CA_0)i_{ur}k_o)N)/((D_0F_0 - 1)r_c^2 + (((AD_0F_0 - A)i_u$$

$$+ 2CA_0D_0F_0 - 2CA_0)k_o$$
$$+ ((\beta_F + \beta_D + \alpha_F + \alpha_D)D_0 - \alpha_D)F_0$$
$$- \alpha_F D_0 - \beta_F - \beta_D)r_c$$
$$+ ((ACA_0D_0F_0 - ACA_0)i_u$$
$$+ CA_0^2D_0F_0 - CA_0^2)k_o$$
$$+ (((A(\alpha_F + \alpha_D)D_0 - A\alpha_D)F_0$$
$$- A\alpha_F D_0)i_u + ((\beta_F + \beta_D$$
$$+ \alpha_F + \alpha_D)CA_0D_0 - \alpha_D CA_0)F_0$$
$$- \alpha_F CA_0D_0 + (-\beta_F - \beta_D)CA_0)k_o) \qquad (14c)$$

$$P_{ooo} = (((AD_0^2F_0^2 - AD_0F_0)i_u + CA_0D_0^2F_0^2 - CA_0D_0F_0)k_o r_c$$
$$+ ((ACA_0D_0^2F_0^2 - ACA_0D_0F_0)i_u + CA_0^2D_0^2F_0^2$$
$$- CA_0^2D_0F_0)k_o^2 + (((A(\alpha_F + \alpha_D)D_0^2 - A\alpha_D D_0)F_0^2$$
$$- A\alpha_F D_0^2F_0)i_u + ((\alpha_F + \alpha_D)CA_0D_0 - \alpha_D CA_0)F_0$$
$$- \alpha_F CA_0D_0)k_o)/((D_0F_0 - 1)r_c^2$$
$$+ (((AD_0F_0 - A)i_u + 2CA_0D_0F_0 - 2CA_0)k_o$$
$$+ ((\beta_F + \beta_D + \alpha_F + \alpha_D)D_0 - \alpha_D)F_0$$
$$- \alpha_F D_0 - \beta_F - \beta_D)r_c$$
$$+ ((ACA_0D_0F_0 - ACA_0)i_u + CA_0^2D_0F_0 - CA_0^2)k_o^2$$
$$+ (((A(\alpha_F + \alpha_D)D_0 - A\alpha_D)F_0 - A\alpha_F D_0)i_u$$
$$+ ((\beta_F + \beta_D + \alpha_F + \alpha_D)CA_0D_0 - \alpha_D CA_0)F_0$$
$$- \alpha_F CA_0D_0 - (\beta_F + \beta_D)CA_0)k_o)$$

$$D_0 = \frac{\alpha_D}{\beta_D + \alpha_D}$$

$$F_0 = \frac{\alpha_F}{\beta_F + \alpha_F}$$

$$CA(0) = CA_0.$$

Together, Eq. 14 form a complete system which can be integrated to determine the bulk cytosolic $[Ca^{2+}]$ during a depolarization of the sarcolemma. The equations depend separately upon the unitary current of the sarcolemmal channel, and upon the open and closed probabilities of the sarcolemmal channel gates. This dependence cannot be reduced to a dependence on the product of the unitary current with the open-probability of the sarcolemmal channel, which is what determines the macroscopic inward calcium current I_{si}. This demonstrates a phenomenon which is common to all "local control" models of calcium-induced calcium release: because of the statistical correlation between the states of individual sarcolemmal and SR calcium channels, bulk SR calcium release is not a unique function of macroscopic I_{si} even though microscopic I_{si} is the only mediator of SR calcium release. Therefore, failure of SR calcium release to show a voltage dependence identical to that of I_{si} does not imply the existence of a direct effect of voltage on the release process.

Eq. 14 leads to calcium transients which display large amplification by SR calcium release, and are nevertheless graded as a function of the size and duration of the trigger depolarization. Fig. 5 shows a family of calcium transients produced by depolarization from a holding potential of −60 mV to a step potential of 0 mV, for durations of 2–50 ms. On the right-hand side of the figure are shown the corresponding transients obtained when SR release is disabled (SR channel conductance set to zero), so that the only source of calcium is the inward current I_{si}. It can be seen that a large amplification factor (nearly 10) is obtained by calcium-induced calcium release, with smooth gradation of the transient as a function of the duration of depolarization. The model is far from being unstable; in fact, because the calcium kinetics of the SR channel are first order, this model cannot produce spontaneous oscillations for physically realizable initial conditions.

This calcium synapse model also displays gradedness as a function of the magnitude of depolarization. The cytosolic $[Ca^{2+}]$ at 50 ms after the onset of depolarization is plotted as a function of the step potential in Fig. 6 *A*. The usual bell-shaped curve is obtained in the absence of SR calcium release, representing the integrated contribution of macroscopic I_{si}, diminished slightly by the effect of ongoing calcium uptake. In the presence of SR release, the smooth bell-shaped gradation with potential is preserved, but with a large amplification by calcium-induced calcium release. In panel *B* of this figure, the separate contributions of I_{si} (*dashed curve*) and SR calcium release (*smooth curve*), have been plotted, normalized to their respective peaks. Superimposing the two

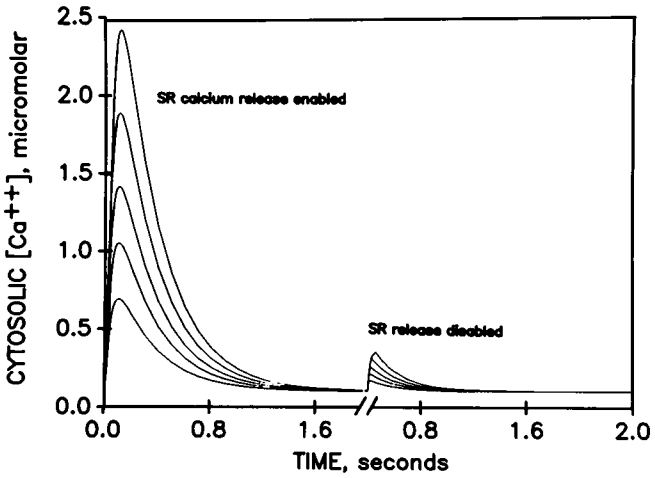

FIGURE 5 Cytosolic $[Ca^{2+}]$ transients generated by the "calcium-synapse" model in response to step depolarizations from −60 to 0 mV lasting 2, 5, 10, 20, and 50 ms. (*Left*) The size of the calcium transients is graded with duration. (*Right*) With SR calcium release turned off, much smaller transients are obtained due to the direct contribution of I_{si}. The numerical values of the model parameters were as follows: r_c = 20, $k_o = 6.67 \times 10^4$, $A = 3 \times 10^{13}$, $P = -10^{-16}$, $i_{ur} = 1.2 \times 10^{-16}$, B = 30, K = 150, $N = 10^{14}$, CA_o = 1 mM, CA_0 = 100 nM, E_0 = 25 mV.

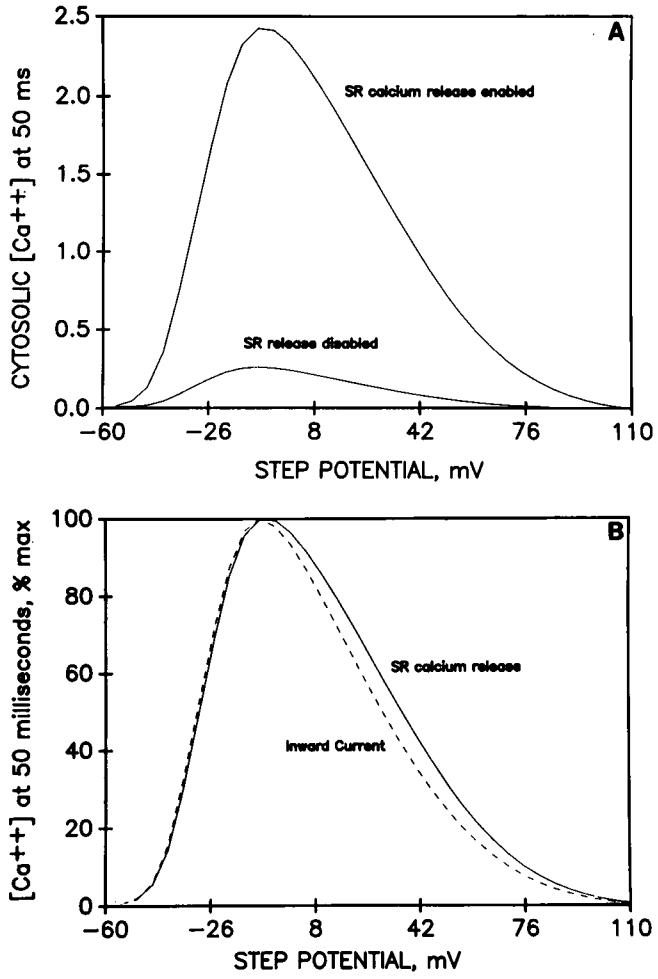

FIGURE 6 (*A*) Cytosolic calcium in the "calcium-synapse" model after a 50-ms depolarization from a holding potential of −60 mV as a function of the step potential, with or without the contribution of SR calcium release. (*B*) The separate contributions of SR calcium release and I_{si}, each normalized to its maximum, showing the difference in their voltage dependences.

contributions in this way reveals that SR release and (cumulated) I_{si} do not have exactly the same voltage dependence, as was predicted above from the structure of Eq. 14. The difference in their voltage dependences (at least for the values of the parameters chosen for this example) is small enough that it would probably not be recognizable in currently available experimental data, so that the observed similarity between I_{si} and $[Ca^{2+}]_{cyto}$ cannot be taken as evidence favoring common-pool over local control models.

"Cluster bomb" models

In local-control models of the "calcium-synapse" type, each sarcolemmal calcium channel is paired with a single SR calcium release channel. The maximum amplification obtainable from SR calcium release is therefore related, in a fundamental way, to the ratio between the unitary currents of the SR and sarcolemmal channels. In order to obtain high amplification, it is necessary to assume unrealistically large conductances for the SR channel. One way to avoid this problem is to assume that a single sarcolemmal channel controls more than one SR channel. Because of the limited range of the calcium diffusion gradient around the sarcolemmal channel pore, the SR channels must be very close to one another, so that they must respond to each other's released calcium. In fact, given the large size of the SR channel protein, the only way that many such channels could be simultaneously controlled by one sarcolemmal channel would be for the signal to be passed from one SR channel to another in "daisy chain" fashion. This leads to the picture of a cluster of SR channels, mutually coupled by their own calcium release, and coupled to one "trigger" sarcolemmal channel. There is ultrastructural evidence that calcium release channels are clustered on the surface of SR release terminals (Ferguson et al., 1984), and dihydropyridine receptors in adult rat ventricle are located predominantly in junctional complexes containing ryanodine receptors (SR release channels) in a stoichiometry of 1:9 (Wibo et al., 1991).

Such a cluster would be locally regenerative, since the closed channels in a cluster are capable of sensing the calcium released from the open channels, being triggered thereby to open in turn. In order to preserve the stability and gradedness of the local-control model, individual clusters must regenerate locally, but be sufficiently separated from one another that no collective ("common-pool") regeneration takes place. We refer to such a model as a "cluster bomb" model.

The simplest cluster bomb model combines the two-gate, four-state (DiFrancesco and Noble) sarcolemmal channel used in the calcium-synapse model with a cluster of two-state SR channels. In order to minimize the probability of the cluster regenerating spontaneously at resting cytosolic calcium concentrations, it is necessary to assume second order (or higher) kinetics for the calcium control of SR channel opening.

As in the calcium-synapse model above, the operation of the cluster-bomb model involves complicated correlations among the stochastic openings of the various channels in the cluster. It is possible, in principle, to write differential equations for the cluster-bomb model by considering all possible "states" of the entire cluster, and determining the transition rates among these states due to the opening or closing of single channels. For a cluster containing 5 SR channels, there are 128 states, whereas for 10 SR channels, the cluster has 4,096 states, making this approach difficult. A somewhat easier approach is Monte-Carlo simulation, in which stochastic transitions are simulated numerically under the control of pseudo-random numbers. The Monte-Carlo algorithm operates as follows. (*a*) Each channel (or gate) in the cluster is assigned a state (0 or 1) describing whether it is open or closed. (*b*) At the beginning of each time step, the probability of opening or closing of the voltage-dependent sar-

colemmal channel gates is computed from the membrane potential. The calcium concentration at each of the closed SR channels is computed by adding the local calcium gradients of all the open channels in the cluster to the background cytosolic calcium. The probability of opening of each SR channel is computed from its local calcium concentration. (*c*) A random number between zero and one is generated for each channel or gate in the cluster. If this number is less than the calculated probability for the channel to open (if closed) or close (if open), then the state of the channel is changed. (*d*) The above steps are carried out for a large ensemble (say 1,000) of independent clusters. The total calcium flux from the ensemble of clusters is used to determine the increment in global cytosolic calcium during the time step, and cytosolic calcium is updated accordingly (including the effect of a relaxation term which steadily removes calcium from the cytosol by a first-order process). (*e*) The sequence of operations above is repeated for a series of small time steps (0.1 or 1 ms), in order to calculate the cytosolic calcium transient as a function of time.

This procedure is straightforward for clusters of any size, but is very intensive computationally. However, the number of computations is roughly proportional to the number of channels in the cluster (summing the local calcium contributions requires a number of steps proportional to the square of the cluster size, but is a small part of the calculation for moderate cluster sizes), whereas the number of variables in the analytical differential equations increases exponentially with the size of the cluster. The Monte-Carlo simulation is therefore easier to implement for realistic cluster models.

In the calcium-synapse model, local regeneration was prevented by the fact that a single SR channel must be either open or closed and so cannot be controlled by its own released calcium. In the cluster-bomb model, on the other hand, collective regeneration of the channels within a cluster does occur. It is therefore necessary to provide a mechanism to "extinguish" the activity of a cluster, once it has been "ignited" by the trigger from the sarcolemmal channel.

There are three mechanisms that can extinguish an active cluster; two of these are exactly analogous to the processes which can terminate regenerative calcium release in a common-pool model, whereas the third is uniquely dependent on the stochastic nature of calcium release by a small cluster of channels.

(*a*) *Calcium-dependent inactivation.* A time-dependent inactivation process, initiated either by the opening of the channel or by the binding of released calcium to a second control site, could terminate release from an active cluster. There is evidence for such a process from the skinned-cell experiments of Fabiato, as discussed above, as well as from studies of calcium release from isolated SR vesicles (Chamberlain, et al., 1984; Meissner and Henderson, 1987). While the early studies of single SR release channels did not demonstrate calcium inactivation, it has recently been observed in bovine cardiac SR channels, using Cs^+ as a charge carrier (Kawano and Coronado, 1991). In studies of isolated SR vesicles or channels, millimolar $[Ca^{2+}]$ was required to strongly inactivate the channel; the presence of physiologic levels of ATP and $[Mg^{2+}]$ was found to shift the $[Ca^{2+}]$ dependence of the release rate markedly to the right, moving the descending limb of the curve (if any) to values very much higher than those observed in Fabiato's experiments, though not necessarily higher than concentrations reached near the pore of the channel itself. All studies of isolated systems have been done in the steady-state, so that the possible activation and inactivation kinetics of the channel in response to rapidly changing $[Ca^{2+}]$ remain unexplored. Simulation of an inactivation process requires including additional states of each SR channel, increasing the computational burden substantially.

(*b*) *Local depletion of releasable calcium.* There is evidence, both physiological and ultrastructural, that SR calcium release sites are located on "release terminals" in the junctional and corbular SR, whereas the calcium uptake pump is located throughout the SR, particularly in the longitudinal SR (Franzini-Armstrong et al., 1985; Jorgensen et al., 1988; Wendt-Gallitelli, 1990), with a significant diffusion resistance to calcium translocation between the uptake and release "compartments" of the SR (Wussling and Szymanski, 1986). If we hypothesize that each cluster draws upon calcium stores in its own release terminal, which are only slowly replenished from the "uptake pool", then "firing" of a cluster will cause local depletion of its releasable calcium. This will reduce the local feedback gain that sustains the activity of the cluster, permitting the channels to close.

(*c*) *Stochastic attrition.* Once activated, a cluster is self-sustaining (in the absence of mechanisms (*a*) and (*b*) above) because the calcium released from open channels is sufficient to promote the opening of closed channels as rapidly as the open channels close. However, this is only true on the average. In a small or moderate sized cluster, there is always a probability that enough channels will close simultaneously to reduce the calcium flux below the self-sustaining level. Once this occurs, the remaining channels will rapidly close, leaving the cluster inactive until it is again triggered. Therefore, active clusters will steadily "die off" spontaneously even in the absence of any extinguishing mechanism, a process we refer to as "stochastic attrition".

The importance of stochastic attrition depends on the size of the cluster and the magnitude of the positive feedback gain sustaining it. For large clusters with high gain, the probability that enough channels will close at once to extinguish the channel becomes very small, leading to essentially macroscopic behavior of the cluster. At the other extreme, if there is only one SR channel, stochastic attrition will completely interrupt the positive feedback process, which is what happens in the calcium-synapse model. For intermediate cluster sizes, stochastic attrition

will make a significant contribution to terminating cluster activity, whether or not extinguishing mechanisms (*a*) and (*b*) are present.

Fig. 7 shows the open-probability of SR calcium channels in clusters of several sizes, starting from a state in which all channels are open, under conditions in which stochastic attrition is the only mechanism affecting cluster activity. The cluster was simulated in the absence of any external trigger or ambient calcium, assuming a single-channel open-state lifetime of 10 ms, an opening rate controlled by calcium according to second order Hill kinetics with a maximum opening rate of 500 s^{-1}, and a Ca_{50} ($[Ca^{2+}]$ producing 50% of the maximal opening rate) equal to twice the $[Ca^{2+}]$ produced by calcium diffusion from one open nearest-neighbor channel. No inactivation or calcium depletion was assumed. For clusters of 10 channels, the rate of stochastic attrition is very small, leading to nearly macroscopic (i.e., latched-up) behavior on the time scale shown. For smaller clusters, stochastic attrition quickly extinguishes all active clusters (in the absence of an external trigger calcium source). For larger or smaller unitary channel currents (relative to the Ca_{50} of the calcium control site), the critical cluster size for stochastic attrition becomes smaller or larger, respectively.

In order to obtain large amplification using SR release channels of modest conductance, it is necessary for the number of channels per cluster to be high enough that stochastic attrition alone is too slow to terminate release by a cluster. In addition, the rate of stochastic attrition is highly sensitive to the exact conditions, which is undesirable. We therefore included local depletion of release terminal calcium stores (mechanism *b* above) in the model simulations, which requires less computation than does channel inactivation.

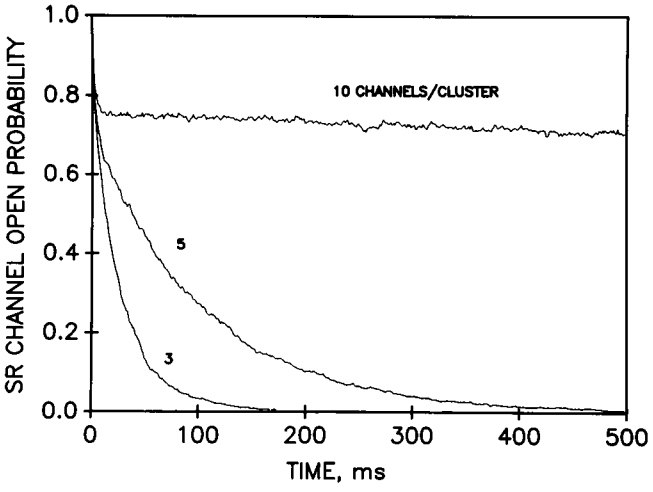

FIGURE 7 Decay of active clusters by stochastic attrition. An ensemble of independent clusters of 3, 5, or 10 channels was modeled in the absence of any background cytosolic calcium or trigger calcium. All channels were started in the open state at $t = 0$. There is an initial rapid decay of the channel-open probability to a quasi-equilibrium value at which the mean calcium released from open channels is sufficient to sustain the average number of open channels. The channel-open probability then continues to fall due to stochastic attrition as entire clusters are extinguished by random fluctuations. The rate of stochastic attrition is very sensitive to the number of channels in a cluster.

For the simulations shown, the kinetics of the sarcolemmal channel were the same as in the calcium-synapse model. The SR release channels were assumed to open at a calcium-dependent rate:

$$r_{open} = r_{max}CA^2/(CA^2 + CA_{50}^2), \qquad (15)$$

where $r_{max} = 100\ s^{-1}$ and $CA_{50} = 20\ \mu M$, and to close at a constant rate $r_{close} = 20\ s^{-1}$. A cluster consisted of a linear array of 5 SR channels separated by 100 nm; the first channel of the array was separated from the sarcolemmal calcium channel by a gap of 6.25 nm. Each open SR channel released calcium at a rate that contributed a local $[Ca^{2+}] = RR \cdot 10\ \mu M$ at a distance of 100 nm (nearest neighbor distance), where RR is a factor to account for local depletion of release terminal calcium stores. The factor RR was updated at each 1-ms time step according to

$$RR' = 0.999RR(1 - 0.01n_{open}) + 0.001, \qquad (16)$$

where n_{open} is the number of open release channels in the cluster; this corresponds to a "restitution" time constant of 1 s. Because of the ill-conditioned numbers involved in representing this process by Eq. 16, computations were done in double-precision. The density of clusters was 10^{14} $liter^{-1}$. Global cytosolic calcium was controlled by the entry of calcium through the various channels in the clusters, with an effective cytosolic volume of 30 times physical volume, to account for buffering. In addition, cytosolic $[Ca^{2+}]$ was subject to a continuous relaxation process with a time constant of 200 ms towards a "resting" (i.e., all channels closed) value of 100 nM, representing the effects of Na/Ca exchange and SR uptake. The actual steady-state $[Ca^{2+}]_{cyto}$ differs only slightly from the resting value, because most channels are closed at the holding potential; because the steady-state value cannot be calculated analytically, the model was started from the resting value and "run in" at the holding potential prior to the step depolarization.

Fig. 8 *A* shows examples of cytosolic calcium transients computed for a cluster model containing 5 SR channels per cluster, during step depolarizations from −60 mV to −15 mV of duration 2, 5, 10, 20, and 50 ms. The choice of −15 mV was made to limit the rapidity of opening of L-type channels, so that a time-step of 1 ms could be used, reducing the computational burden. Panel *B* of this figure shows the corresponding transients in the absence of SR calcium release, i.e., including the direct contribution of the inward calcium current alone. It can be seen that nearly 10-fold amplification by calcium-induced calcium release is achieved, with release graded as a function of the duration of depolarization.

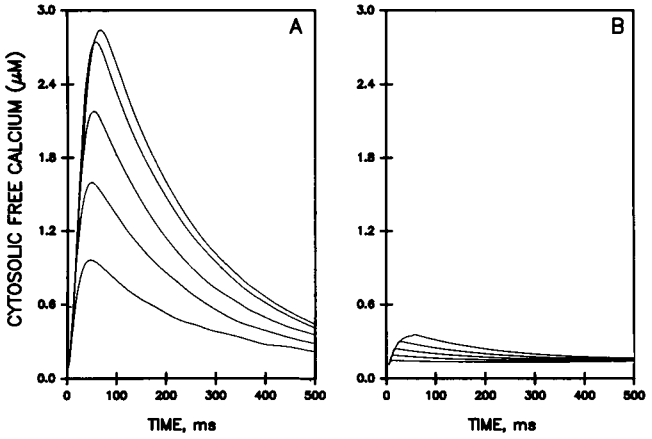

FIGURE 8 Calcium transients ($[Ca^{2+}]_{cyto}$, μM) generated by the "cluster-bomb" model for step depolarizations from −60 to −15 mV for 2, 5, 10, 20, or 50 ms. The curves in *A* were generated with SR calcium release present, while those in *B* had the unitary current of the SR channel set to zero to display the contribution of the inward calcium current alone. The step potential of −15 mV (rather than 0 as in Fig. 9) was chosen because the slower rate of activation of the L-type channel activation gate permitted larger time steps, reducing the computational burden. Qualitative features are the same at other step potentials.

This was accomplished with an assumed SR channel unitary current only 2.5 times the maximum unitary current of the sarcolemmal calcium channel, as compared with the example shown in Fig. 5 for the calcium-synapse model, which used an SR channel 23 times larger than the sarcolemmal channel. Note, by comparing the two panels of Fig. 8, that the variation of the SR release component of the calcium transient with the duration of depolarization is not the same as that of the inward current component, even though the system is not globally regenerative. This cannot be considered "nonlinearity", because, as discussed above, in local-control models the SR calcium release is not directly a function of the macroscopic inward calcium current.

This point is further emphasized by the voltage dependence of the calcium transient, which is compared, in Fig. 9, with that of the inward current component alone, both being normalized to their respective maxima. Although the curves are somewhat noisy, it is clear that SR release deviates from the inward current trigger at high step potentials. Interestingly, for the parameters used here, the deviation is in the opposite direction from that seen in the calcium-synapse model (Fig. 6 *B*). The results of the Monte-Carlo simulation can be made arbitrarily smooth by averaging sufficiently many iterations. However, the noise decreases only as the inverse square root of the number of iterations, and Fig. 9 already represents 2×10^{11} computer instructions.

The classic bell-shaped curve of the inward calcium current represents a trade-off between the number of sarcolemmal calcium channels activated, which increases with the step potential, and the unitary current of these channels, which falls towards zero as the step potential increases towards the calcium reversal potential. Despite the similarity between the voltage dependences of SR calcium release and the inward current, the discrepancy between these two curves is actually a clue to the fact that the number of sarcolemmal channels activated, on the one hand, and the magnitude of their unitary current, on the other, play fundamentally different roles in controlling calcium release in the cluster-bomb model.

To understand this, it is useful to visualize how calcium release is graded in the cluster-bomb model. Once a cluster is activated, it will regenerate more-or-less autonomously. The gradation of calcium release is therefore largely a reflection of the recruitment of varying numbers of active clusters. When the sarcolemma is depolarized, the rate of recruitment of clusters will be controlled by a rate-limiting stochastic event, which may be either the first opening of the sarcolemmal trigger channel or the opening of a critical number of SR cluster channels after they have been exposed to trigger calcium. The rate of first-opening of the sarcolemmal channel is an increasing function of membrane potential, whereas the rate of opening of the SR channels depends on the magnitude of the trigger calcium, i.e., on the unitary current of the triggering sarcolemmal channel, which is a decreasing function of potential. As the step potential is made more positive, the rate limiting step in recruitment crosses over from the sarcolemma to the SR. The exact voltage at which this crossover occurs would be expected to depend on the distance between the sarcolemmal channel and the SR channels, the regenerative gain of the cluster, and the rates of activation and deactivation

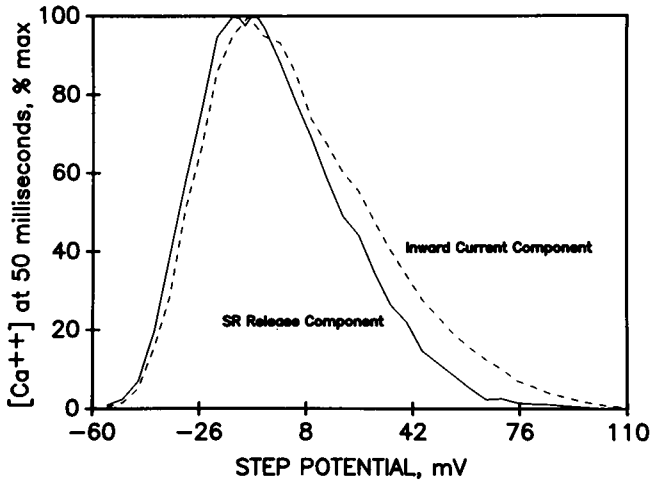

FIGURE 9 Normalized contributions of SR calcium release and I_{si} to the cytosolic calcium increase at the end of a 50-ms step depolarization from a holding potential of −60 mV in the "cluster bomb" model, as a function of the step potential. Both I_{si} and SR calcium release have a bell-shaped variation with membrane potential, but their voltage dependence is not the same, even though microscopic I_{si} is the triggering stimulus for SR calcium release. Calculation was by the Monte-Carlo algorithm, using a time-step of 100 μs.

of the SR channels as a function of local $[Ca^{2+}]$. Most of this parameter space remains to be explored, because of the large amount of computation required. In general, however, the position of the ascending and descending limbs of SR calcium release as a function of voltage need not be same as those of the macroscopic inward current, even though the microscopic inward current is the only signal triggering SR calcium release.

THEORY OF THE PROPAGATED CALCIUM WAVE

It is well known that so-called "calcium overload" of myocytes causes periodic spontaneous release of calcium from the sarcoplasmic reticulum, and that this release propagates as a "calcium wave" traveling at a velocity of the order of 100 μm/s (see Stern et al. [1988] for a review of this phenomenon). It is reasonable to assume that the occurrence of these calcium oscillations, or at least their propagation, is due to regeneration of the calcium-induced calcium release machinery of the SR, although this is by no means proven, as discussed above. If this machinery involves local control by the sarcolemmal calcium channel, then when it regenerates in response to global cytosolic calcium it is not operating as "intended" by its designer. Nevertheless, at constant membrane potential (particularly at the resting potential), the local coupling of sarcolemmal calcium channels to the SR channels will have no effect, and the cell should behave as a common-pool system. This is manifested experimentally by the lack of an effect of L-type channel blockers on spontaneous calcium waves in resting hearts or myocytes, (Stern et al., 1989).

In keeping with our use of modeling as an aid to understanding rather than an attempt to simulate the detailed behavior of the cell, we will analyze the principles behind the regenerative propagation of calcium-induced calcium release using several highly idealized models of the wave that can be solved analytically. The aim will be to understand how the qualitative features of SR calcium release determine the relationship between wave amplitude and velocity, the shape of a calcium wave and, particularly, the conditions under which such a wave may fail to propagate.

Observed properties of propagated calcium waves

Quantitative experimental data on the propagated wave are still rather sparse. The calcium profile of the wave has been imaged (Takamatsu and Wier, 1990; Berlin et al., 1989), but quantum noise limits the precision with which the leading edge of the wave can be resolved. Wave velocities have been measured in papillary muscles and single myocytes (Kort et al., 1985; Takamatsu and Wier, 1990); they tend to fall within a rather narrow range of 80–120 μm/s. Macroscopic waves have been observed to propagate for millimeters at velocities of up to 15 mm/s in intact trabeculae immediately after rapid stimulation under conditions of marked calcium loading; these have been modeled as due to calcium-induced calcium release (Backx et al., 1989) but this required extreme assumptions about parameters, including diastolic calcium high enough to saturate calcium buffers, and it is not clear that these propagated aftercontractions represent the same phenomenon as the waves in single myocytes. Wave velocity in myocytes increases with the product of extracellular calcium and inter-wave interval (M. Capogrossi, personal communication) which is a surrogate for SR calcium content. One might think, therefore, that the narrow range of wave velocities is accounted for by the fact that most observed waves are initiated by spontaneous calcium release, and therefore tend to occur at about the same critical level of SR calcium loading. To study wave propagation over a wider range of SR calcium loads, one would like to initiate waves externally in cells that are not spontaneously oscillating. This can be done by means of subthreshold field stimulation, local application of caffeine, or localized photo-release of caged calcium, (M. Capogrossi, personal communication; O'Neill et al., 1990). When this is attempted, however, the waves commonly fail to propagate or die out after a short distance. Indeed, even waves that are spontaneously initiated at one end of a calcium-loaded cell are often observed to die out before traversing the entire length of the cell. It appears, therefore, that cells which can generate a robust twitch, and even cells displaying spontaneous SR calcium release, are nonetheless rather refractory to the propagation of calcium waves. This is the principal paradox which we seek to understand theoretically.

The details of the construction of analytical models of wave propagation lie somewhat outside the field of excitation-contraction coupling per se, and are presented in the Appendix. The principal conclusions are as follows.

(*a*) If it is assumed that SR calcium release sites are effectively homogeneously distributed, the wave may be modeled as a continuum process, with cytosolic $[Ca^{2+}]$ governed by the diffusion equation, supplemented by a source term representing the flux of calcium exchanged locally with the SR and other organelles. By assuming a solution in the form of a wave propagating steadily in one dimension, an integral equation is derived which determines the wave velocity and shape. This equation can be solved numerically, given a model for the SR calcium release dynamics. By representing SR calcium release at a more phenomenalogical level by a "Maxwell's demon" who watches $[Ca^{2+}]_{cyto}$ and decides when to trigger SR release, it is possible to solve for the wave analytically, and study the effect of different types of triggering algorithms on wave propagation. In general, there exists a minimum rate of SR Ca^{2+} release required to sustain propagation of the wave, and a corresponding nonzero minimum propagation velocity. For a variety of models of threshold triggering, this refractory condition

is only reached for waves whose amplitude is comparable to the threshold for triggering release, i.e., much smaller than the systolic $[Ca^{2+}]$ transient. However, if the triggering of SR release is made highly sensitive to the rate of rise of $[Ca^{2+}]_{cyto}$, then a high degree of refractoriness can be obtained, consistent with the observations. In this case, the primitive Maxwell's demon model successfully predicts the observed range of wave velocities, without adjustable parameters.

(*b*) If release terminals are distributed inhomogeneously within the sarcomere, computation of the wave is much more complex. It is possible to idealize the situation by placing a threshold-triggered SR release site exactly at each Z-line, obtaining an analytically soluble model. This model shows that sarcomeric localization itself can produce a high degree of refractoriness, due to the loss of $[Ca^{2+}]_{cyto}$ (by uptake and extrusion) as it diffuses across the "firebreak" of inexcitable SR between release regions. In this model, the degree of refractoriness is quite sensitive to sarcomere length, which should be testable experimentally.

DISCUSSION

The analyses presented above demonstrate that it would not be a simple matter to explain the macroscopic features of cardiac excitation-contraction coupling, even if the properties of the calcium release channel were fully known. None of the models presented above, complex as they are, purports to be a realistic model, i.e., one that could be used to simulate experiments quantitatively. Yet each of them embodies features which seem to be required in order to explain observed properties of cardiac E-C coupling. To recapitulate briefly, experiments demonstrate that the cardiac calcium transient is tightly coupled to the inward calcium current, yet other experiments show that, under conditions not too far removed from physiological, spontaneous and propagated calcium release occur as all-or-none phenomena. We have demonstrated that it is improbable that this state of affairs can be explained by a homogeneous model, i.e., one in which a common cytosolic pool of calcium provides the pathway for all calcium transactions among the sarcoplasmic reticulum, the sarcolemma and the myofilaments. At present, this demonstration falls somewhat short of a proof. In the linear case, we have proven that a large amplification (defined in terms of the area of the calcium transient) by means of calcium-induced calcium release is incompatible with robust stability of the equilibrium state. In order to rule out common pool models entirely, it would be necessary to show experimentally that a large amplification is present under conditions in which the trigger is small enough that the system behaves linearly, and that the resting state of such a cell can be perturbed in the direction of increased calcium release without leading to oscillations.

Avoiding common pool models means, by definition, subdividing the calcium pool architecture of the cell in some way. We have chosen to analyze models in which this is done by placing the sarcolemmal calcium channel in close proximity to SR calcium release channels, because there is ultrastructural evidence for such an arrangement in mammals, as well as recent physiologic evidence that calcium from the sarcolemmal channel is more effective in releasing calcium from the SR than calcium entering by Na/Ca exchange (Sham et al., 1992). Our analysis shows that coupling by local $[Ca^{2+}]$ diffusion gradients can give rise to high amplification of the inward calcium current without requiring so much positive feedback as to lose the graded character of SR release. Interestingly, avian myocytes lack t-tubules but have extensive SR release terminals, the majority of which do not make junctional couplings with the sarcolemma (Sommer, 1991). These cells show gradation of SR release in skinned-cell experiments (Fabiato, 1982), but it is not known whether intact avian myocytes show graded release in response to a wide range of depolarization conditions, as do mammalian cells.

There are a great variety of local control models possible, depending on the kinetics of the SR and sarcolemmal channels and the geometry of their relationship to one another. We have analyzed only the simplest models of two classes (single channel and cluster), over a limited range of parameters, and have left out many important phenomena, such as calcium inactivation of the sarcolemmal and SR channels and realistic kinetics of the SR calcium uptake pump. More detailed and realistic analysis of local control models, and fitting of their parameters to experimental data, will require extensive computational resources. In order to limit the range of possibilities, it will be necessary to have good data about the kinetics of individual SR channels in isolation. Single channel studies done so far show that there are several open and closed states of the channel, indicating that more complex channel models will be needed. These studies also show that the sensitivity of the SR channel to calcium varies over several orders of magnitude as a function of the cytosolic concentrations of magnesium and ATP. It is critically important that detailed channel gating statistics be studied at physiological concentrations of these ligands, which has not yet been done (indeed, it is not entirely certain what the physiologic level of Mg^{2+} is).

In principle, if the channel is Markovian, knowledge of the transition rates among all of its states in the presence of steady levels of cytosolic calcium would make it possible to calculate its behavior in the presence of time-varying calcium concentrations. In practice, if there are many closed states, this may be difficult to do, because there may be rapid transitions among multiple closed states which are difficult to detect in the steady-state but are important under dynamic conditions. It would therefore be very desirable to measure channel statistics in response to step changes of calcium. For example, the

experiments of Fabiato (1985*b*), as well as the theoretical analysis of the propagated wave above, indicate that macroscopic SR calcium release depends on the rate of rise of trigger calcium. The physical implementation of this "rate detection" probably involves a fast competition between activation and inactivation. It is possible that the very low sensitivity of the SR channel to steady levels of calcium in the presence of physiologic concentrations of magnesium is actually a reflection of rapid passage through an open state to an inactivated state, so that much smaller concentrations of calcium would suffice to open the channel if applied rapidly. Alternatively, this low sensitivity may be physiologic if the channel normally functions in a local-control configuration in which it is exposed to high local concentrations of trigger calcium.

A further gap in our knowledge of SR channel kinetics concerns the lifetime of the open state(s) as a function of calcium. As indicated above, there is disagreement in the literature as to whether the closure rate is influenced by ambient calcium. Actually, none of the published results may be relied upon, because the studies were done using EGTA in submillimolar concentrations as a calcium buffer. The calcium off-rate k_{-1} for EGTA is only 1 s^{-1}, and its affinity K is $\sim 10^{-6}$ M. The average time for a calcium ion released from the channel pore to bind to EGTA is given by $K/k_{-1}[\text{EGTA}])$ which is ~ 10 ms at an EGTA concentration of 100 μM. The time required for the ion to diffuse 34 nm (the diameter of the SR channel) is given by r^2/D, where $r = 34$ nm, which gives ~ 1.1 μs. Therefore, the chance that calcium released from the SR channel pore interacts with EGTA before reaching the calcium sensing site on the channel is negligible, and the local free calcium gradient is essentially unbuffered. In order to measure the open state lifetime without interference from feedback calcium, much faster diffusible calcium buffers must be used in millimolar concentrations; even in this case buffering will be marginal (Stern, 1992).

If the propagated calcium wave is interpreted as a manifestation of the calcium-induced calcium release machinery, it provides another constraint on whatever model is finally chosen. Wave propagation requires sufficient common-pool gain (under conditions of "calcium overload") and convex dependence of release rate on $[Ca^{2+}]$. The common-pool properties of the SR would best be measured by doing calcium-step or calcium-clamp experiments while measuring cytosolic calcium. Recent improvements in caged-calcium compounds, together with the development of calcium-sensing dyes that are optically compatible with them, offers hope that this will soon be possible. It is quite possible, of course, that the SR release sites are heterogeneous, some being low affinity sites closely coupled to sarcolemmal calcium channels, whereas others are free standing, high affinity sites. Such a composite model would provide a great many free parameters to help in papering over the apparent conflicts presented by different classes of physiological experiments. In order to convincingly validate such a model, much more experimental evidence on the ultrastructural localization of calcium release will be needed.

Although calcium-induced calcium release has been shown convincingly to be the mechanism of cardiac excitation-contraction coupling, further understanding of complex spatial relationships among calcium transport and release sites is essential before the operation of this mechanism can be said to be understood.

APPENDIX

Models of propagation of the calcium wave

Continuum models of calcium waves

We assume that the calcium wave propagates by diffusion of calcium from the wave front, which triggers calcium-induced calcium release from the SR ahead of the wave. As an idealized model, we consider a wave propagating steadily in one dimension along a cell of infinite length (in fact, longitudinal waves in cardiac myocytes do quickly develop a plane front and propagate at constant velocity). We will assume that the sites of calcium release and uptake are continuously distributed throughout the cytosol, and that calcium buffering can be represented as linear and instantaneous, increasing the effective volume of distribution of cytosolic calcium by a factor B. The magnitude of B can be estimated to be ~ 30 (over the range of $[Ca^{2+}]$ from 0 to 1 μM) by adding up the various known calcium buffers in the cell (Fabiato, 1983). Calcium uptake from the cytosol will be assumed to be a first order process with rate constant kB, i.e., k (s^{-1}) is the rate constant for relaxation of cytosolic free calcium. Under these assumptions, the deviation of cytosolic $[Ca^{2+}]$ from equilibrium, which we call $x(t, z)$, is governed by a diffusion equation with added terms for uptake and release of calcium:

$$B\frac{\partial x}{\partial t} = D\frac{\partial^2 x}{\partial z^2} - kBx + R\{x(t, z)\}, \qquad (17)$$

where z is the longitudinal spatial coordinate along the length of the cell and D is the diffusion coefficient of free calcium in the cytosol.

The release term $R\{x(t, z)\}$ depends on $x(t, z)$ and the history of $x(t, z)$ according to some dynamical model governed by differential equations that could be written if we knew the kinetics of the release channel and the dynamics of SR calcium compartments. Since we are looking for a solution that has the form of a wave propagating at constant velocity without change of shape, we specify that the solution has the form $x = x(t - z/v)$, where v is the (as yet unknown) velocity of the wave. Putting this into Eq. 17, and setting $z = 0$, gives:

$$(D/Bv^2)\frac{dx^2}{dt^2} - \frac{dx}{dt} - kx + R(t)/B = 0, \qquad (18)$$

which is an ordinary differential equation for $x(t)$, the (departure from equilibrium of) $[Ca^{2+}]$ as a function of time at one point in space as the wave goes by.

If we pretend that the release term $R(t)$ is known, then Eq. 18 is a second order linear differential equation with constant coefficients and a source term. This equation can be solved by Laplace transform methods, and if we specify that the solution must vanish for large positive and negative times, i.e., before the wave arrives and after it has passed, we obtain the following equation:

$$e^{\lambda_+ t}\int_t^\infty e^{-\lambda_+ t'}R(t')\,dt' + e^{\lambda_- t}\int_{-\infty}^t e^{-\lambda_- t'}R(t')\,dt' = B\left\{\frac{4Dk}{Bv^2}+1\right\}^{1/2}x \quad (19a)$$

$$\lambda_+ = \frac{vB\{(v^2+4Dk/B)^{1/2}+v\}}{2D} \quad (19b)$$

$$\lambda_- = -\frac{vB\{(v^2+4Dk/B)^{1/2}-v\}}{2D}, \quad (19c)$$

where the exponential rate constants λ_+ and λ_- are positive and negative, respectively.

For large negative and positive times, where $R(t)$ vanishes, $x(t)$ will in fact fall to zero at these exponential rates. In order to be sure of this, $R(t)$ must vanish faster than the exponentials, i.e., faster than $x(t)$ on which it actually depends. This can be insured by requiring that $R(t)$ be the nonlinear part of the release. In other words, we assume that any part of the release term which is linear in $x(t)$ has already been taken out of R and included in the linear uptake term, giving an effective uptake coefficient k. Since we assume that the equilibrium state before the arrival of the wave is stable, the effective k must be positive. Fig. 10 shows schematically the extraction of the nonlinear part of release for the case of a release rate that is controlled instantaneously by cytosolic $[Ca^{2+}]$ according to first or second order kinetics. Note that for the case of first order kinetics, the nonlinear part of "release" is actually negative. Examining Eq. 19, all the terms other than R are positive. Therefore, in order to sustain a steadily propagated wave, the dependence of SR release on trigger calcium must be second order or higher.

In order to obtain analytically soluble models, we now assume that the control of SR release can be described phenomenalogically by various "Maxwell's demon" devices. For example, we may assume that

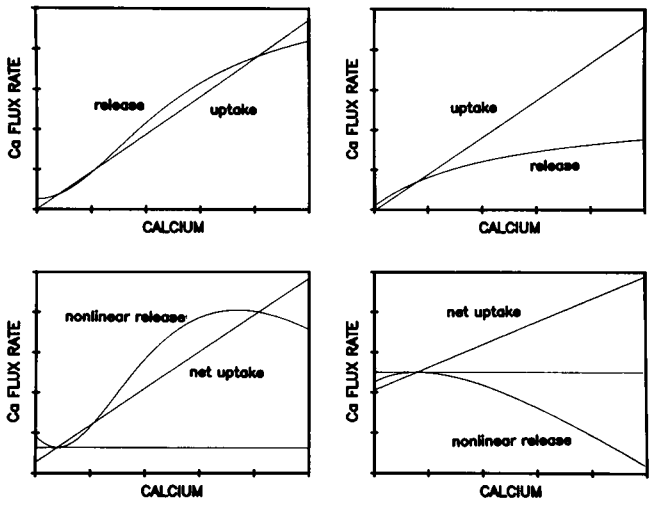

FIGURE 10 Schematic example of the extraction of the nonlinear part of calcium release, as required in the analysis of the propagating calcium wave. The upper panels show calcium release (*smooth curve*) and uptake (*straight line*) as a function of cytosolic calcium for SR channels instantaneously controlled by $[Ca^{2+}]$. On the left side, SR calcium release is a second order Hill function of $[Ca^{2+}]$; in the right side it is first order. The equilibrium point is where the two curves intersect in each panel; the difference between the curves is net calcium release. In the lower two panels, the linear part of release (i.e., a straight line tangent to the release curve at the equilibrium point) has been subtracted from the release curve, giving nonlinear release, and from the linear uptake curve, giving an effective uptake rate. The horizontal lines are at zero, showing that the nonlinear part of release is positive for second (and higher) order release, but always negative for first order release.

the Maxwell's demon controlling the SR waits until it is exposed to a threshold level of calcium x_0, and then initiates a release of calcium at an initial rate r, decaying exponentially, i.e., $R(t) = r\exp(-t/\tau_r)$. Of course, the "threshold" and time course imposed by the Maxwell demon are actually determined by the dynamics of the SR channels interacting with the local calcium concentration, but, for purposes of this schematic model, we will treat them as though they are known "after the fact," in order to obtain analytical models that reveal the roles that these parameters play in controlling propagation velocity and refractoriness. Since the wave could arrive at any arbitrary time, we are at liberty to assume that $t = 0$ is the time at which threshold is reached and release begins. Inserting this form for $R(t)$ into Eq. 19, and requiring that $x(t) = x_0$ at $t = 0$, we obtain the following equation determining the release rate r in terms of the threshold trigger calcium x_0 and the exponential rate constant λ_+ of the "toe" of the approaching wave, which is defined by Eq. 19b to be a positive, increasing function of wave velocity v:

$$r = \frac{B(\lambda_+ + 2k)(\lambda_+\tau_r + 1)x_0}{\lambda_+\tau_r}. \quad (20)$$

This equation may be regarded as implicitly determining the wave velocity (which is a unique function of λ_+, found by inverting Eq. 19b) when the SR release rate and trigger threshold have been specified. The release rate r has a minimum value r_m as a function of λ_+, which may be found by differentiating Eq. 20:

$$r_m = B\frac{\left\{\left(\frac{2k}{\tau_r}\right)^{1/2}+2k\right\}\left(\frac{\tau_r}{2k}\right)^{1/2}\left\{\left(\frac{2k}{\tau_r}\right)^{1/2}\tau_r+1\right\}x_0}{\tau_r}. \quad (21)$$

Therefore, there is a minimum calcium release rate below which no steady wave propagation is possible, i.e., the cell is refractory to calcium waves (note that this has nothing to do with refractoriness to electrical conduction of the action potential at the sarcolemma). For calcium release rates greater than r_m there are two possible values of λ_+ (and therefore of velocity v) that satisfy Eq. 20. One of these lies on the ascending limb on which r is an increasing function of v, and represents a physically possible solution. The other lies on the limb where velocity decreases as the calcium release rate increases, and represents an unstable, nonphysical situation. The physical solutions therefore lie on the ascending limb of Eq. 20, so that for any release rate above r_m there will be a steady wave traveling at a velocity greater than v_m, the velocity of the limiting wave at release rate r_m. There is, therefore, a nonzero minimum velocity of propagated waves, given by:

$$v_m = \left\{\frac{2Dk/B}{\left\{\left(\frac{2k}{\tau_r}\right)^{1/2}+k\right\}\tau_r}\right\}^{1/2}. \quad (22)$$

The failure of a wave to propagate when the SR calcium release rate is too low can be described in terms of the notion of safety factor. The $[Ca^{2+}]$ at the peak of a wave must be sufficient to diffuse forward, losing some calcium to uptake, and still reach threshold to trigger release from the adjacent SR. The ratio of the peak $[Ca^{2+}]$ of the wave to the threshold is the safety factor for sustained propagation of the wave; it must exceed some minimum value greater than 1 for the wave to be sustained. To determine safety factor, it is useful to plot wave velocity against peak calcium x_p rather than release rate r as the independent variable. We determine x_p as follows: the time dependence of calcium in the wave, $x(t)$, is determined from Eq. 19 after substituting the values of $R(t)$ and v and performing the integrals. By setting the derivative of $x(t)$ to zero, we can solve for the time at which the wave peaks, and substitute this time in $x(t)$ to find the peak calcium, x_p as a function of r. Solving for r in terms of x_p and substituting back into Eq. 20, an expression is found relating wave velocity v to wave amplitude x_p, parameters that are experimentally accessible. This equation, which is very complicated, will not be reproduced here.

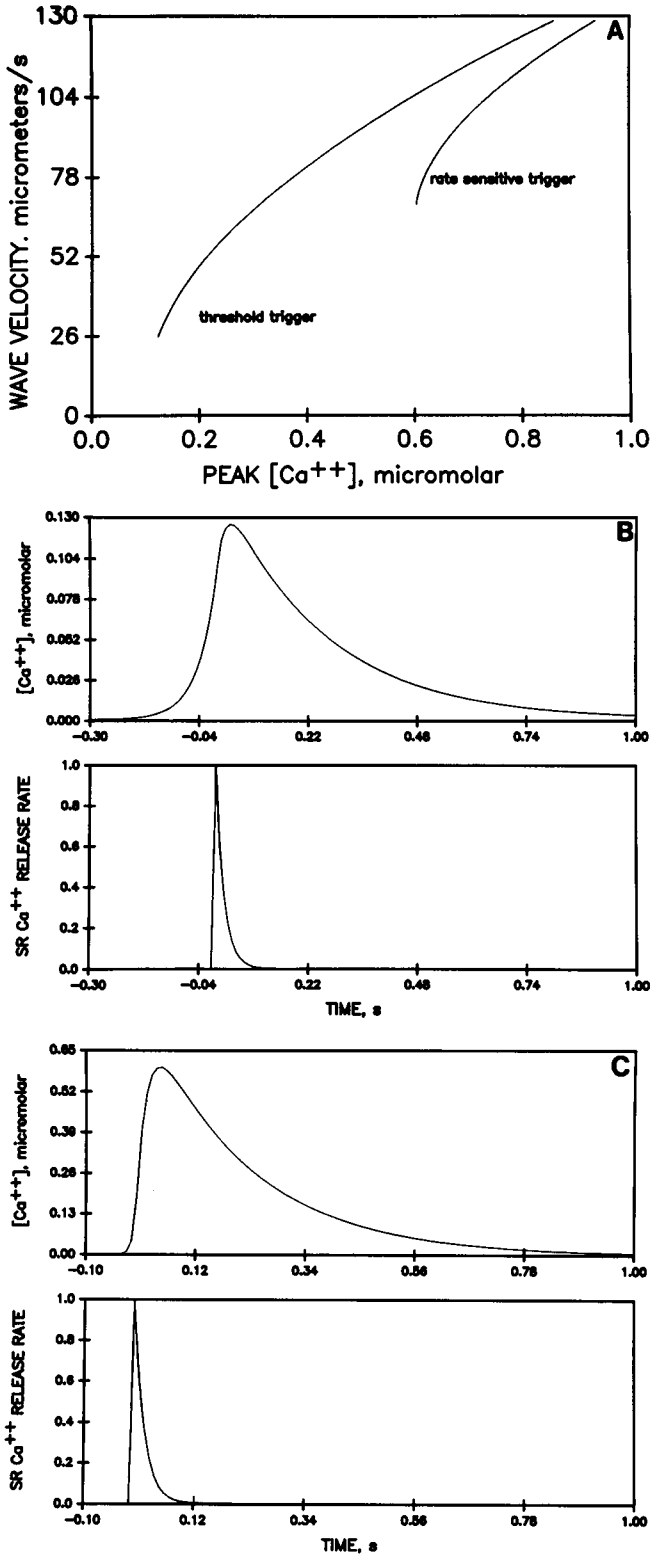

FIGURE 11 (*A*) Velocity of the continuum-model calcium wave as a function of wave amplitude (i.e., peak $[Ca^{2+}]$). The left-hand curve shows the model in which SR calcium release is triggered when cytosolic $[Ca^{2+}]$ reaches 0.1 μM, and decays exponentially with a time constant of 10 ms. In the right-hand curve, the triggering condition is that $[Ca^{2+}]$ has increased by 0.1 μM over the value 5 ms previously. No propagated waves exist with lower amplitudes or velocities than the leftmost points of the curves. (*B* and *C*) The time course of cytosolic $[Ca^{2+}]$ (at one point in space) for the smallest possible propagated wave. *B* is for threshold-triggered release, corresponding to the leftmost point of the left-hand curve in *A*. *C* is for rate-sensitive triggering (leftmost point of the right-hand curve in *A*). The upper curves are $[Ca^{2+}]$ (note the difference in scale between *B* and *C*), whereas the lower curves show normalized SR calcium release rate.

This relationship between wave amplitude and velocity is plotted as the left-hand curve in Fig. 11 *A*. The threshold x_0 was taken to be 0.1 μM, based on the studies of Fabiato (1983, 1985) in which a calcium step was rapidly applied to skinned myocyte fragments to trigger calcium release. The diffusion coefficient D was taken to be 10^{-5} cm^2/s, the value for calcium ion free in solution. Note that D is the free calcium diffusion coefficient, and should not be affected by the presence of calcium buffers.

As the curve shows, there exist a minimum amplitude and velocity for wave propagation; however, both appear to be rather small compared with what is observed experimentally. Based on the theory, the occurrence of refractoriness for waves of the same order of magnitude as the systolic twitch ($\sim$1 μM) would not be expected. The minimum safety factor x_p/x_0 for propagation is only modestly greater than 1. In Fig. 11 *B*, the smallest propagating wave is displayed. It has a peak amplitude only a little over threshold, and a slow rise. The timing of $[Ca^{2+}]$ in relation to SR calcium release is somewhat counterintuitive. Most of the rise in calcium occurs by passive diffusion from the oncoming wavefront. SR release begins only as the wave is about to go by, and most of the released calcium goes to feed the forward propagation of the wave, rather than to increase local calcium.

This highly schematic Maxwell demon model captures the phenomenon of wave propagation by diffusion-triggered calcium-induced calcium release, and even produces wave velocities of the correct order of magnitude without adjustment of parameters. However, it does not display the high degree of refractoriness seen experimentally. In order to explain this paradox, the first consideration is whether we have chosen our threshold correctly. The value of x_0 was based on the studies of Fabiato in skinned cells, but it is much lower than the trigger calcium concentrations which would be present at the SR release channel in a local-control model. We must consider the possibility that the safety factor of the waves which are observed, experimentally, to die out may not actually be high.

We need, first, to understand the meaning of "threshold" in the phenomenalogical model. Since, in our interpretation, the sarcolemmal calcium channel plays no role in wave propagation, the local calcium balance during wave propagation in a resting cell will be controlled in the same manner as in a common-pool model. In the resting cell, before wave initiation, cytosolic calcium will lie at a stable equilibrium value at which (slight) release is balanced by SR uptake. If this value is increased beyond a critical value, a local regenerative release will ensue; the amount of calcium which must be added to reach this critical point corresponds to the "threshold" in the Maxwell-Demon model. As cell calcium loading is raised, a point will be reached at which the resting equilibrium point itself becomes unstable; this coincides with the onset of spontaneous oscillations. As this degree of calcium loading is approached, the increment in cytosolic calcium required to move from the (barely stable) equilibrium point to an unstable state will approach zero. Therefore, when the cell is calcium-loaded nearly to the point of oscillation, the threshold for triggering regenerative release will be very small. This argument applies regardless of the actual calcium affinity of the SR channel. Even if the channel is very insensitive (having been designed for local control), when the SR is loaded sufficiently the apparent threshold for triggering bulk calcium release will be small. This is because, under these conditions, only a small fraction of SR channels needs to be opened to trigger regeneration.

The above considerations help to rationalize the observation of Fabiato that bulk SR calcium release can be triggered by a 0.1-μM calcium increment with the possibility that the SR channel actually has a

low affinity for calcium, which would be expected in a local-control model (and is observed in single channel studies in the presence of physiological levels of free magnesium). This further emphasizes the paradoxical nature of the failure of spontaneous waves to propagate. If the cell is calcium loaded to the point where actual oscillation is initiated at one end of the cell, then the effective threshold for triggering release from adjacent areas, which must be loaded nearly to the point of oscillation, ought to be very low, and the safety factor for propagation should be very high (for example, if the peak $[Ca^{2+}]$ of the wave is 1 μM and the threshold is 0.1 μM, the safety factor is 10). Yet spontaneous waves are often observed to die out.

One possibility that we considered was to introduce a delay or "latency" between the sensing of threshold calcium and the initiation of release, to simulate the time dependence of channel kinetics. In the presence of latency, release would only begin after the wave was already passing by, and would have to be larger in order to "catch up". Without presenting the details here, it suffices to say that the inclusion of latency reduces the calculated velocities (particularly for large waves) and increases refractoriness rather modestly. So long as the time constant for relaxation is long compared with the latency time and to the duration of SR calcium release, the critical safety factor for propagation is not increased much above 1.

Another possibility is that release is actually triggered from within the SR, by calcium which has been taken up from the approaching wavefront. This would increase the SR calcium concentration to a critical threshold at which the SR spontaneously releases calcium, thereby passing the wave along to adjacent SR. Analysis of this scheme, by methods similar to those above, shows that there is a minimum total amount of released SR calcium required for propagation to occur. This minimum release size is equal to twice the difference between the resting SR content and the threshold for spontaneous release (the factor of two arises because the released calcium diffuses equally in both forward and backward directions). There is, however, no minimum wave velocity. The wave velocity goes to infinity as the resting SR load approaches the threshold for spontaneous release. It does so sufficiently slowly, however, that achieving velocities higher than those observed in myocytes would require the resting SR to be loaded to over 99.9% of the threshold for spontaneous release. In that condition it would be very difficult to distinguish rapid propagation from multifocal spontaneous release. Once again, this model provides no mechanism by which a cell on the verge of spontaneous calcium release could be refractory to wave propagation.

To exclude the possibility that the lack of refractoriness is due to the oversimplified nature of the Maxwell-Demon mechanism, we solved numerically for propagation velocity when SR release was represented by a detailed channel-kinetics scheme. The diffusion Eq. 18 was augmented by providing a set of differential equations governing the state variables (SR calcium stores and channel states) controlling the release term R. These equations were solved with trial values of the velocity, which was adjusted iteratively to satisfy Eq. 19. Fig. 12 shows wave velocities calculated from such a model, as a function of the resting cytosolic $[Ca^{2+}]$ at which the cell is equilibrated. The SR model used was a rather complicated four-state model, including calcium-dependent inactivation and latency in channel opening, which was designed to reproduce the calcium inactivation experiments of Fabiato. This model will not be discussed in detail here, because many of its features have probably been rendered obsolete by the isolation of the SR release channel. The significant point is that such a detailed model gives wave velocity-calcium relationships qualitatively similar to those produced by the Maxwell demon model, and shows no evidence of refractoriness until calcium loading is reduced far below the level of at which spontaneous oscillation occurs.

We have found only one mechanism in a continuum model that can produce the kind of refractoriness observed. This is the inclusion of a strong dependence of SR triggering on the rate of rise of cytosolic calcium. This can be modeled by assuming that the condition for triggering the Maxwell demon is that the rise in calcium during the immediately preceding time interval Δt is equal to the threshold, i.e., $x(t) - x(t - \Delta t) = x_0$. With this condition, x_0 is still the threshold that would be observed in an experiment such as that of Fabiato, in which cytosolic calcium was increased suddenly by micro-injection around the SR.

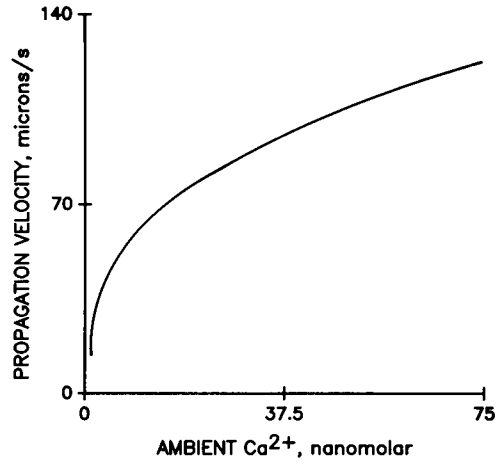

FIGURE 12 Wave velocity versus resting cytosolic calcium for a "realistic" continuum model based on a four-state SR release channel with calcium-dependent activation and inactivation, designed to mimic the skinned cell experiments of Fabiato (1983, 1985*a, b, c*). The rightmost point corresponds to the resting cytosolic calcium at which "spontaneous" calcium oscillations set in. The leftmost point gives the minimum wave which is capable of propagating. Refractoriness appears only at calcium loads well below the point of spontaneous release.

This model can be analyzed in a manner exactly analogous to Eqs. 20–22. The degree of refractoriness is found to increase as the "sensing time" Δt is made shorter. The right-hand curve in Fig. 11 *A* shows the relationship between wave amplitude and velocity for Δt = 5 ms, with all other parameters the same as for the left-hand curve. The wave velocity for large waves is similar to that found in the absence of rate-sensing, but the minimum wave amplitude and velocity for propagation are much higher. The critical wave which just manages to propagate is shown in Fig. 11 *C;* it is larger and has a steeper front than was seen in the absence of rate-dependent triggering. It should be noted that the range of velocities found agrees very well with the range observed in isolated myocytes, even though no effort was made to adjust the parameters to fit these velocities. The significance of this agreement should not be overstated, because the proper values for the free-calcium diffusion coefficient D and the cytosolic calcium buffering B are not known with precision, and the time dependence of buffering has not been taken into account.

Spatially discrete models of the calcium wave

The preceding analysis of the propagated wave assumed that SR calcium release and uptake sites are continuously distributed throughout the cytosolic space. Actually, ultrastructural evidence suggests that release sites are concentrated near the Z-line of the sarcomere. Such localization could strongly influence the propagation of a calcium wave, because released calcium must diffuse across a "firebreak" of passive cytosol in order to reach and trigger the release sites in the adjacent sarcomere.

The salient effects of localization of release sites can be demonstrated by a relatively simple, idealized model that can be solved analytically. In this model, SR release sites are located exactly at the Z-line. When cytosolic calcium at a Z-line reaches the threshold x_0, a fixed amount of calcium BLx_{max} is instantaneously released at the Z-line, and begins diffusing away, subject to instantaneous buffering and first order uptake as in previous models. In this formulation, L is the sarcomere length and x_{max} is the peak cytosolic calcium that would be reached if

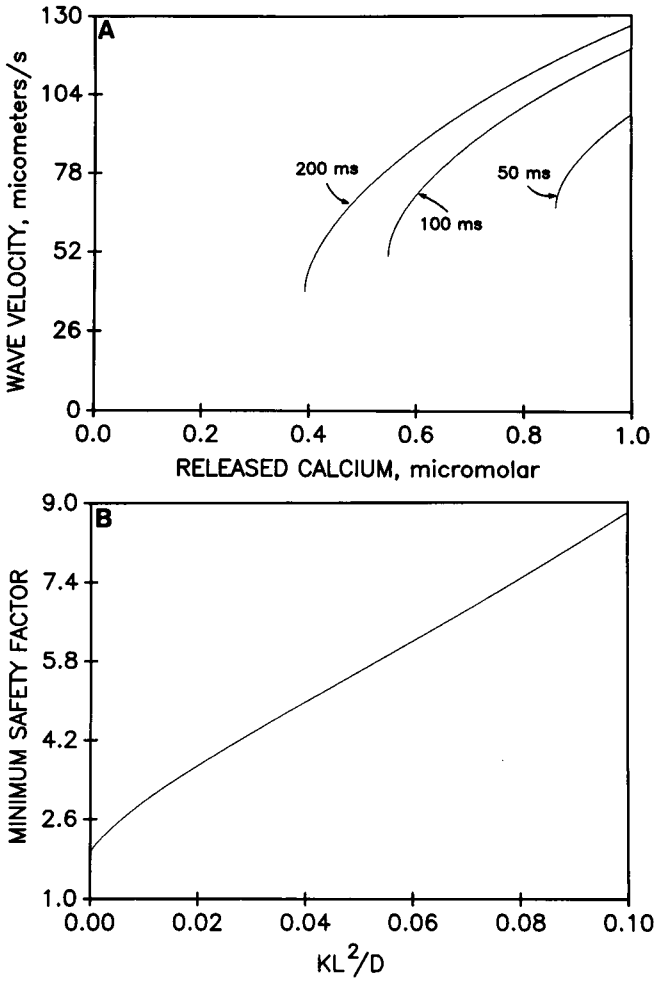

FIGURE 13 Propagated calcium wave in a model with discrete localization of SR release sites at the Z-line of the sarcomere. (*A*) Velocity of the wave as a function of released calcium (expressed as equivalent free calcium when distributed uniformly over the sarcomere), for three different values of the calcium relaxation (reuptake) time constant $1/k$. (*B*) The minimum safety factor required for propagation as a function of the "dimensionless uptake rate" kL^2/D, where L is sarcomere length and D is the free calcium diffusion coefficient.

the released calcium were instantly distributed uniformly throughout the sarcomere.

The concentration, at location z and time t, of a unit amount of calcium released at $z = z_0$, $t = t_0$ is found by solving the diffusion equation with a linear uptake term:

$$x = \frac{\left\{\frac{B}{\pi D(t-t_0)}\right\}^{1/2} e^{-[B(z-z_0)^2/4D(t-t_0)]-k(t-t_0)}}{2}. \quad (23)$$

We assume that a wave is traveling from left to right at velocity v, so that the release site at $z = 0$ reaches threshold x_0 at time $t = 0$. The nth release site to the left of $z = 0$ will then be located at $z = -nL$, and will have released its calcium at $t = -nL/v$. Summing the diffusing calcium fronts (each given by Eq. 23) from all these release sites, and requiring that the resulting calcium equal the threshold x_0 at $z = 0$, $t = 0$, we obtain:

$$x_{max} = \frac{2\pi^{1/2}x_0/L}{\left\{\frac{Bv}{DL}\right\}^{1/2} \sum_{n=1}^{\infty} \frac{e^{-Ln(Bv^2+4Dk)/4Dv}}{n^{1/2}}}, \quad (24)$$

which is an equation (implicitly) determining the velocity v as a function of x_{max}. Using this equation, the wave velocity is plotted against "wave amplitude" x_{max} in Fig. 13 *A*, assuming a sarcomere length of 2.2 μm, for several values of the uptake time constant $1/k$. The value of x_{max} is a surrogate for wave amplitude, which is not well defined because the actual time course of calcium during the passage of a wave will be different at each point in the sarcomere. As seen in this figure, there is substantial refractoriness compared with the continuum model without rate sensing. This occurs because a wave will fail to propagate if the time required for calcium to diffuse from one sarcomere to the next is sufficient for a large fraction of that calcium to be taken up from the cytosol. In Fig. 13 *B*, the minimum safety factor for propagation, x_{max}/x_0, is plotted as a function of the "dimensionless uptake rate" kL^2/D.

This "simple" model shows that localization of the SR release sites within the sarcomere could explain the high degree of refractoriness of calcium waves seen experimentally. Since the "dimensionless uptake rate" is proportional to the square of sarcomere length, the degree of refractoriness should increase rather sensitively as sarcomere length is increased. This might provide an experimental test of the importance of release site localization. To our knowledge, there is no data regarding this possibility in cardiac myocytes, which are usually studied at slack length ($L \approx 1.9$ μm). However, calcium waves are routinely observed in unstimulated rat papillary muscles stretched to the length for maximum force production (Kort et al., 1985).

Received for publication 27 September 1991 and in final form 6 April 1992.

REFERENCES

Adler, D., A. Y. K. Wong, Y. Mahler, and G. A. Klassen. 1985. Model of calcium movements in the mammalian myocardium: interval-strength relationship. *J. Theor. Biol.* 113:379–394.

Ashley, R. H., and A. J. Williams. 1990. Divalent cation activation and inhibition of single calcium release channels from sheep cardiac sarcoplasmic reticulum. *J. Gen. Physiol.* 95:981–1005.

Backx, P. H., P. P. de-Tombe, J. H. Van-Deen, B. J. Mulder, and H. E. ter-Keurs. 1989. A model of propagating calcium-induced calcium release mediated by calcium diffusion. *J. Gen. Physiol.* 93:963–977.

Barcenas-Ruiz, L., and W. G. Wier. 1987. Voltage dependence of intracellular $[Ca^{2+}]_i$ transients in guinea pig ventricular myocytes. *Circ. Res.* 61:148–154.

Beuckelmann, D. J., and W. G. Wier. 1988. Mechanism of release of calcium from sarcoplasmic reticulum of guinea-pig cardiac cells. *J. Physiol. (Lond.)*. 405:233–255.

Berlin, J. R., M. B. Cannell, and W. J. Lederer. 1989. Cellular origins of the transient inward current, I_{TI}, in cardiac myocytes: role of fluctuations and waves of elevated calcium. *Circ. Res.* 65:115–126.

Block, B. A., T. Imagawa, K. P. Campbell, and C. Franzini-Armstrong. 1988. Structural evidence for direct interaction between the molecular components of the transverse tubule/sarcoplasmic reticulum junction in skeletal muscle. *J. Cell Biol.* 107:2587–2600.

Cannell, M. B., J. R. Berlin, and W. J. Lederer. 1987. Effect of membrane potential changes on the calcium transient in single rat cardiac cells. *Science (Wash. DC)*. 238:1419–1423.

Chamberlain, B. K., P. Volpe, and S. Fleischer. 1984. Calcium-induced calcium release from purified cardiac sarcoplasmic reticulum vesicles. *J. Biol. Chem.* 259:7540–7546.

Cleemann, L., and M. Morad. 1991. Role of Ca^{2+} channel in cardiac excitation-contraction coupling in the rat: evidence from Ca^{2+} transients and contraction. *J. Physiol. (Lond.)*. 432:283–312.

DiFrancesco, D., and D. Noble. 1985. A model of cardiac electrical activity incorporating ionic pumps and concentration changes. *Phil. Trans. R. Soc. Lond.* 307:353–398.

Fabiato, A. 1982. Calcium release in skinned cardiac cells: variations with species, tissues, and development. *Fed. Proc.* 41:2238–2244.

Fabiato, A. 1983. Calcium-induced release of calcium from the cardiac sarcoplasmic reticulum. *Am. J. Physiol.* 245:C1–C14.

Fabiato, A. 1985*a*. Rapid ionic modifications during the aequorin-detected calcium transient in skinned canine cardiac Purkinje cell. *J. Gen. Physiol.* 85:189–246.

Fabiato, A. 1985*b*. Time and calcium dependence of activation and inactivation of calcium-induced release of calcium from the sarcoplasmic reticulum of a skinned canine cardiac Purkinje cell. *J. Gen. Physiol.* 85:247–289.

Fabiato, A. 1985*c*. Simulated calcium current can both cause calcium loading in and trigger the calcium release from the sarcoplasmic reticulum of a skinned cardiac Purkinje cell. *J. Gen. Physiol.* 85:291–320.

Fabiato, A. 1985*d*. Spontaneous versus triggered contractions of "calcium-tolerant" cardiac cells from the adult rat ventricle. *Basic Res. Cardiol.* 80(Suppl 2):83–87.

Fabiato, A. 1989. Appraisal of the physiological relevance of two hypothesis for the mechanism of calcium release from the mammalian cardiac sarcoplasmic reticulum: calcium-induced release versus charge-coupled release. *Mol. Cell. Biochem.* 89:135–140.

Ferguson, D. G., H. W. Schwartz, and C. Franzini-Armstrong. 1984. Subunit structure of junctional feet in triads of skeletal muscle: a freeze-drying, rotary-shadowing study. *J. Cell Biol.* 99:1735–1742.

Franzini-Armstrong, C., and D. G. Ferguson. 1985. Density and disposition of Ca^{2+}-ATPase in sarcoplasmic reticulum membrane as determined by shadowing techniques. *Biophys. J.* 48:607–615.

Hilgemann, D. W., and D. Noble. 1987. Excitation-contraction coupling and extracellular calcium transients in rabbit atrium: reconstruction of basic cellular mechanisms. *Proc. R. Soc. Lond.* 230:163–205.

Jones, L. R., and S. E. Cala. 1981. Biochemical evidence for functional heterogeneity of cardiac sarcoplasmic reticulum vesicles. *J. Biol. Chem.* 256:11809–11819.

Jorgensen, A. O., R. Broderick, A. P. Somlyo, and A. V. Somlyo. 1988. Two structurally distinct calcium storage sites in rat cardiac sarcoplasmic reticulum: an electron microprobe analysis study. *Circ. Res.* 63:1060–1069.

Kauffmann, R., R. Bayer, T. Furniss, H. Krause, and H. Tritthart. 1974. Calcium movement controlling cardiac contractility. II. Analogue computation of cardiac excitation-contraction coupling on the basis of calcium kinetics in a multicellular compartmental model. *J. Mol. Cell. Cardiol.* 6:543–559.

Kawano, S., and R. Coronado. 1991. Ca^{2+} dependence of Ca^{2+} release channel activity in the sarcoplasmic reticulum of cardiac and skeletal muscle. *Biophys. J.* 59:600*a*. (Abstr.)

Kort A. A., M. C. Capogrossi, and E. G. Lakatta. 1985. Frequency, amplitude, and propagation velocity of spontaneous Ca^{++}-dependent contractile waves in intact adult rat cardiac muscle and isolated myocytes. *Circ. Res.* 57:844–855.

Lai, F. A., H. P. Erickson, E. Rousseau, Q. Liu, and G. Meissner. 1988. Purification and reconstitution of the calcium release channel from skeletal muscle. *Nature (Lond.)*. 331:315–319.

Meissner, G., and J. S. Henderson. 1987. Rapid calcium release from cardiac sarcoplasmic reticulum vesicles is dependent of Ca^{2+} and is modulated by Mg^{2+2}, adenine nucleotide and calmodulin. *J. Biol. Chem.* 262:3065–3073.

Nabauer, M., G. Callewaert, L. Cleemann, and M. Morad. 1989. Regulation of calcium release is gated by calcium current, not gating charge, in cardiac myocytes. *Science (Wash. DC)*. 244:800–803.

New, W., and W. Trautwein. 1972. The ionic nature of slow inward current and its relation to contraction. *Pfluegers Arch.* 334:24–38.

Niggli, E., and W. J. Lederer. 1990. Voltage-independent calcium release in heart muscle. *Science (Wash. DC)*. 250:565–568.

ONeill, S. C., J. G. Mill, and D. A. Eisner. 1990. Local activation of contraction in isolated rat ventricular myocytes. *Am. J. Physiol.* 258:C1165–C1168.

Rousseau, E., J. S. Smith, and G. Meissner. 1987. Ryanodine modifies conductance and gating behavior of single Ca^{2+} release channel. *Am. J. Physiol.* 253:C364–C368.

Rousseau, E., and G. Meissner. 1989. Single cardiac sarcoplasmic reticulum Ca^{2+}-release channel: activation by caffeine. *Am. J. Physiol.* 256:H328–H333.

Schouten, V., L. Cleemann, P. Pancha, and M. Morad. 1988. Modeling of excitation-contraction coupling in heart muscle. *Biophys. J.* 53:604*a*. (Abstr.)

Sham, J. S. K., L. Cleeman, and M. Morad. 1992. Gating of cardiac release channel: role of sodium current and sodium-calcium exchange. *Science (Wash. DC)*. 255:850–853.

Sommer, J. R., E. Bossen, and R. Nassar. 1991. Avian extended JSR (EJSR): a challenge to direct contact signal transduction (DCT) for coupling excitation to calcium-release (ECR) in cardiac muscle. *Physiologist.* 34:109.

Stern, M. D., M. C. Capogrossi, and E. G. Lakatta. 1984. Propagated contractile waves in isolated cardiac myocytes modeled as regenerative calcium induced calcium release from the sarcoplasmic reticulum. *Biophys. J.* 45:940*a*. (Abstr.)

Stern, M. D., M. C. Capogrossi, and E. G. Lakatta. 1988. Spontaneous calcium release from the sarcoplasmic reticulum in myocardial cells: mechanisms and consequences. *Cell Calcium.* 9:247–256.

Stern, M. D., H. F. Weisman, D. G. Renlund, G. Gerstenblith, O. Hano, P. Blank, and E. G. Lakatta. 1989. Laser backscatter studies of intracellular Ca^{2+} oscillations in the isolated heart. *Am. J. Physiol.* 257:H665–H673.

Stern, M. D. 1992. Buffering of calcium in the vicinity of a channel pore. *Cell Calcium.* 13:183–192.

Takamatsu, T., and W. G. Wier. 1990. Calcium waves in mammalian heart: quantification of origin, magnitude, waveform, and velocity. *FASEB (Fed. Am. Soc. Exp. Biol.) J.* 4:1519–1525.

Talo, A., M. D. Stern, H. A. Spurgeon, G. Isenberg, and E. G. Lakatta. 1990. Sustained subthreshold-for-twitch depolarization in rat single ventricular myocytes causes sustained calcium channel activation and sarcoplasmic reticulum calcium release. *J. Gen. Physiol.* 96:1085–1103.

Wendt-Gallitelli, M. F., and G. Isenberg. 1989. X-ray microanalysis of single cardiac myocytes frozen under voltage-clamp conditions. *Am. J. Physiol.* 256:H574–H583.

Wibo, M., G. Bravo, and T. Godfraind. 1991. Postnatal maturation of excitation-contraction coupling in rat ventricle in relation to the subcellular localization and surface density of 1,4-dihydropyridine and ryanodine receptors. *Circ. Res.* 68:662–673.

Wier, W. G., and D. T. Yue. 1986. Intracellular calcium transients underlying the short-term force-interval relationship in ferret ventricular myocardium. *J. Physiol. (Lond.)*. 376:507–530.

Wong, A. Y. K. 1981. A model of excitation-contraction coupling of mammalian cardiac muscle. *J. Theor. Biol.* 90:37–61.

Wong, A. Y. K., A. Fabiato, and J. B. Bassingthwaighte. 1987. Model of Ca release mechanism from the sarcoplasmic reticulum: Ca-mediated activation, inactivation and reactivation. *In* Electromechanical, Activation, Metabolism and Perfusion of the Heart: Simulation and Experimental Models. S. Sideman and R. Beyar, editors. Dordrecht, Martinus Nijhoff. 281–295.

Wussling, M., and G. Szymanski. 1986. Simulation by two calcium store models of myocardial dynamic properties: potentiation, staircase, and biphasic tension development. *Gen. Physiol. Biophys.* 5:135–152.